



University of Texas at Tyler
Scholar Works at UT Tyler

Mechanical Engineering Theses

Mechanical Engineering

Fall 12-14-2019

INTEGRATED DESIGN APPROACH FOR CORONARY STENTS USING FLEXINOL SHAPE MEMORY ALLOY

Matthew Lucci
University of Texas at Tyler

Follow this and additional works at: https://scholarworks.uttyler.edu/me_grad

 Part of the [Mechanical Engineering Commons](#)

Recommended Citation

Lucci, Matthew, "INTEGRATED DESIGN APPROACH FOR CORONARY STENTS USING FLEXINOL SHAPE MEMORY ALLOY" (2019). *Mechanical Engineering Theses*. Paper 10.
<http://hdl.handle.net/10950/2316>

This Thesis is brought to you for free and open access by the Mechanical Engineering at Scholar Works at UT Tyler. It has been accepted for inclusion in Mechanical Engineering Theses by an authorized administrator of Scholar Works at UT Tyler. For more information, please contact tgullings@uttyler.edu.



INTEGRATED DESIGN APPROACH FOR CORONARY STENTS USING
FLEXINOL SHAPE MEMORY ALLOY

by

MATTHEW LUCCI

A thesis submitted in partial fulfillment
of the requirements of the degree of
Master of Science in Mechanical Engineering
Department of Mechanical Engineering

Chung Hyun Goh, Ph. D., Committee Chair

College of Engineering

The University of Texas at Tyler
Fall 2019

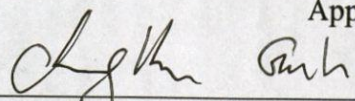
The University of Texas at Tyler
Tyler, Texas

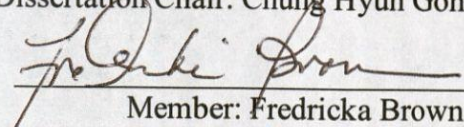
This is to certify that the Master's Thesis of

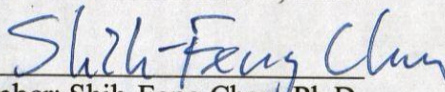
MATTHEW LUCCI

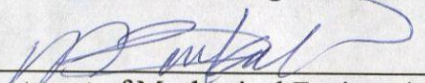
has been approved for the thesis requirement on
November 8th, 2019
for the Master of Science in Mechanical Engineering degree

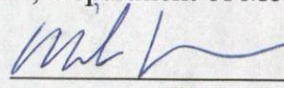
Approvals:


Thesis/Dissertation Chair: Chung Hyun Goh, Ph.D.


Member: Fredricka Brown, Ph.D.


Member: Shih-Feng Chou, Ph.D.


Chair, Department of Mechanical Engineering

 For JK
Dean, College of Engineering

© Copyright by Matthew Lucci 2019

All rights reserved

Dedication

I would like to dedicate my research to those that have supported me along the long journey. Their unconditional love and constant encouragement have made me not only a better academic, but also a better person. It is my hope that this thesis serves to advance academic research to save lives in the intervention of cardiovascular diseases and makes proud all of those that have impacted the course of this research.

Acknowledgments

I would like to express my sincere gratitude toward those that made this possible. First and foremost, I thank God for His blessings in my life and His providence during the research process. Thank you to countless friends and family for encouragement and love through hard times. Without all of your support and the strength, this work would not be what it is today. Thank you, Mom and Dad, for your support in everything that I do. Thank you to my siblings for their encouragement and affection: Benjamin, Rebekah, Rachel, Jacob, Isaiah, and Hezekiah.

I would also like to thank my graduate advisor, Dr. Chung Hyun Goh, for providing academic support throughout the process of developing this thesis. My thesis committee, including Dr. Fredricka Brown and Dr. Shih-Feng Chou, provided invaluable resources for my research. Further thanks to Joseph Oyedele for his support and assistance in this research.

Additionally, I am grateful to Dr. Dennis Cali, Dr. Dennis Robertson, Professor Vanessa Joyner, and the entire UT Tyler debate program for their role in bringing me to the University of Texas at Tyler to pursue graduate studies. Without them, and Dr. Ben Voth of Southern Methodist University, none of this would have been possible.

Table of Contents

List of Tables	iii
List of Figures	iv
Abbreviations	v
Abstract	vi
Chapter 1. Introduction	1
1.1 Overview	1
1.2 Research Objective	9
1.3 Research Question	9
1.4 Working Hypothesis	10
1.5 Tasks	10
1.6 Organization of Thesis	12
 Chapter 2. Behavior of Flexinol Wire.....	13
2.1 Introduction.....	13
2.2 Literature Review.....	14
2.3 Mathematical Formulation of the Resistive Behavior of Standard Metals.....	17
2.4 Mathematical Formulation of the Resistive Behavior of Flexinol.....	23
2.5 Experimental Validation	32
2.6 Closure and future work.....	37
 Chapter 3. Flexinol Stent as a Self-Expanding Bare Metal Stent.....	39
3.1 Introduction	39
3.2 Literature Review	43
3.3 Design Approach	46
3.4 Results and Discussion	48
3.5 Closure and future work	52
 Chapter 4. Blood Flow through Flexinol Stent.....	54
4.1 Introduction.....	54
4.2 Literature review	55
4.3 Mathematical Simulation of Blood Flow.....	61
4.4 CFD Model Setup and Validation.....	65
4.5 Results and Discussion	68
4.6 Concluding remarks and future work	71

Chapter 5. Conclusions and Future Work72

 5.1 Key Results 72

 5.2 Application of Machine Learning 73

 5.3 Closure 74

References 77

Appendices87

 Appendix A: Stress-dependent Flexinol Wire Actuation 87

Biographical Sketch90

List of Tables

Table 1. Average material properties of Flexinol wire sample	22
Table 2. Numerical values for Flexinol constants.....	23
Table 3. Parameters of Flexinol phase change.....	26
Table 4. Numerical values for Flexinol phase change parameters.....	27

List of Figures

Figure 1. Process workflow of tasks.	11
Figure 2. Plot of Resistance Curves for Martensite (Blue) and Austenite (Red) Phases..	28
Figure 3. Plot of Resistance Curves with Linear Transformation Assumption.	29
Figure 4. Experimental Setup.....	32
Figure 5. Current vs. wire diameter for various operating conditions.	33
Figure 6. Resistance versus strain in Flexinol wire sample.	35
Figure 7. Plot of resistance related to strain.	36
Figure 8. Stent design in SolidWorks.	47
Figure 9. Boundary conditions and meshing in SolidWorks.	49
Figure 10. Von Mises stress in the stent when subjected to normal loading conditions...	50
Figure 11. Displacement of the stent under normal loading conditions.	51
Figure 12. Schematic overview of in-stent restenosis.....	56
Figure 13. CFD model validation.	66
Figure 14. Computer-aided design models of each artery case	67
Figure 15. Static pressure distribution for the healthy artery case.....	68
Figure 16. Static pressure distribution for stenosed artery case.....	69
Figure 17. Static pressure distribution for stented artery case.	69

Abbreviations

BMS	Bare Metal Stent
BRS	Bioresorbable Stent
CAD	Computer-Aided Design
CFD	Computational Fluid Dynamics
DES	Drug-Eluting Stents
FEA	Finite Element Analysis
ISR	In-Stent Restenosis
PCI	Percutaneous Coronary Intervention
SMA	Shape Memory Alloy

Abstract

INTEGRATED DESIGN APPROACH FOR CORONARY STENTS USING FLEXINOL SHAPE MEMORY ALLOY

Matthew Lucci

Thesis Chair: Chung Hyun Goh, Ph.D.

The University of Texas at Tyler
October 2019

This research seeks to develop and verify a model for control of the shape memory alloy (SMA) Flexinol and apply such findings to practical application of the material as a platform for bare metal stenting technologies. Utilizing experimental data and material properties, a mathematical model of the thermoelectric contraction behavior of Flexinol wire samples was developed. This model accounted for variable resistance due to the shape memory effect of the Flexinol wire as it experiences a crystalline phase change. It also accounted for the change in the cross-sectional area of the wire as the wire experienced thermal expansion and contraction. The resulting constitutive equations were verified via experimentation.

This thesis further expanded upon these models and presented the practical application of the SMA Flexinol as a platform for coronary artery stenting technologies. The research presented includes computer-aided design (CAD) modeling and finite element analysis (FEA) simulation of the stress loads when working conditions are applied, which revealed the response behavior of the proposed stent design. With the FEA verification that the Flexinol stent design will be able to sustain normal working conditions once implanted into the human body, it was demonstrated that the proposed low stress design has the potential to reduce the rate of stent failure and restenosis in comparison to typical technologies available on the market.

Computational fluid dynamics (CFD) methods were implemented to study the blood flow patterns and associated fluid-structure interaction through the implanted Flexinol stent. The CFD solutions demonstrated the stent's impact on restoring the flow of blood through a stenosed artery to that of a healthy artery. The simulations also showed minimal turbulence in the stented region, which corresponds to lower stresses in the arterial wall and a reduced likelihood of thrombosis as compared to typical stent designs, providing substantial benefit to patients undergoing emergency surgery for the implantation of arterial stents.

This research serves as the basis for the implementation of the SMA Flexinol in engineering applications, particularly those in the biomedical fields. The constitutive equations for Flexinol wire are applicable to a nearly infinite set of SMA applications. The expanded analysis of the SMA stenting application demonstrated the ability for the controllable thermoelectric contraction behavior of Flexinol to be used for more accurate implantation of SMA stents in the human body. The impacts of this research include an

impending breakthrough in the treatment of coronary artery disease with a reduction in the common complications of thrombosis and restenosis. Future research will build upon the crucial work presented in this thesis and will grow from the successful development of the Flexinol stent technology presented herein.

Chapter 1

Introduction

1.1 Overview

With coronary artery diseases as the leading cause of death in the developed world [1] [2], there is a tremendous necessity for research into methods of prevention and treatment of these critical conditions. Even as technology advances in many sectors of biomedicine, treatments for cardiovascular diseases have undergone only incremental improvements that have had any significant impact on the affected population. The evidence suggests that such a substantial disease requires new and innovative solutions to drive a positive change in biomedical technology to treat these conditions. This thesis serves as the basis for research into such a new and innovative technology that has the potential to save countless lives.

To understand the tremendous impact of coronary artery diseases, it is necessary to consider the life-threatening symptoms of the condition. Cardiovascular diseases are the most frequent cause of death worldwide [1] [2]. Among these, coronary artery disease is the most common and the deadliest [3]. Much of this is due to abnormal blood flow and related complications caused by constricted arteries [4]. Coronary artery disease is caused by the collection of fatty plaque along the inside of the artery, also called the tunica interna, resulting in the narrowing of the said artery [3]. Fatty plaque build-up is common as people age but can become severe with certain lifestyle habits, making this an especially dangerous disease in western countries [5]. This build-up of plaque and corresponding

narrowing of the arterial tube is referred to as “atherosclerosis,” and can lead to a complete blockage of the artery. In small arteries, such blockages can cause a critical nutrient depletion in the affected area. In larger arteries, this can lead to death. In most cases, there is a lack of symptoms until the artery is dangerously blocked, allowing only a small stream of blood to flow through [6].

Even plaque build-ups that do not completely block the flow of blood can be extremely dangerous. For example, plaques can break away from the wall and enter the bloodstream or cause damage to the vessel wall. If these conditions are left untreated, plaque can make the artery vulnerable to rupture, resulting in myocardial infarction and potentially fatal stroke [7]. As such, it is important for affected patients to pursue effective treatment as soon as possible. It is critical that advanced methods of treatment be available to provide a variety of effective options and ensure the highest possible rate of patient survival.

Of the widely available methods currently on the market, there are a few that warrant not only a mention, but brief consideration to serve as the foundation for the advanced stenting technology presented in this thesis. Advanced forms of cardiovascular disease often require a revascularization procedure to restore the flow of blood to affected tissues [7]. There are two primary methods through which this is accomplished; vascular or coronary bypass, and angioplasty. In vascular bypass, plaque blockages are surgically bypassed to restore blood flow through a grafted section of artery [8]. For angioplasty treatment, also known as percutaneous coronary intervention (PCI), a catheter is inserted into the blood vessel with a tiny deflated balloon that is then inflated to re-open the blocked or collapsed artery [9]. There are several methods of performing this procedure, including

implanting coronary artery stents to hold the artery open for an extended period of time. It is this procedure that is of interest in this research.

Implantation of coronary stents is a common method of treatment for patients with a variety of cardiovascular diseases [10]. It is estimated that over 6 million coronary stents are implanted into patients each year [11]. Coronary stents are mesh-like tubes inserted into blocked and/or constricted arteries to reopen them and allow for adequate blood flow [12]. This procedure can be life-saving. Surgery to implant stents can be a dangerous and expensive procedure, depending on the amount of blockage, difficulty in maneuvering the stent to the deployment location, and the specific model of the stent [3]. Rapid development of stent technologies in recent decades has led to their widespread use as an emergency treatment for stenosed arteries [7]. PCI with stents has fundamentally changed the way that coronary artery disease is treated around the world and has been used in millions of life-saving procedures [13].

While new methods have been developed in recent years, balloon angioplasty is the most common method of implanting coronary stents and is considered to be a minimally invasive procedure. In this procedure, a crimped stent is placed upon a tiny balloon that is inserted into a constricted artery and then inflated to expand the stent to expand the arterial wall [3]. Plaque that is present in the artery during the procedure is compressed between the expanded stent and the tunica interna. With this process, the stented artery increases in diameter to a size greater than the surrounding artery, which can cause challenges to selecting the correct stent model and size [14]. Improper selection of stent types and sizes can lead to medical complications that require additional procedures to correct.

Due to the severity of heart diseases and the benefits of treatment with coronary stents, coronary stent implantation has become a standard method of treatment for PCIs, as this method of coronary dilation provides better patient outcomes than balloon angioplasty alone [9] [15]. Because of this, it is imperative to design stents that can be self-expandable and avoid typical balloon angioplasty altogether. This thesis presents the development of coronary artery stents that are designed to be self-expandable and controllable with the option of insertion without balloon angioplasty, which is still the most common method of revascularization.

Even with current technology, there exists a risk that an implanted coronary stent could contract over time due to improper placement, causing the blood vessel to constrict, a condition called restenosis [16]. Another condition caused by improper placement of a coronary stent is called thrombosis, on which the stent causes clotting of blood within the stent, potentially requiring emergency surgery to remove the stent [17] [18]. In addition to these, there are a variety of additional conditions and complications associated with improperly placed or non-biocompatible stents, including neointimal hyperplasia, inflammation, and abnormal blood flow [19]. Each of these conditions can develop into potentially fatal issues, and ought to be considered during the development of advanced stenting technologies.

In this thesis, the shape memory alloy (SMA) Flexinol is used as the basis for an advanced stenting platform in order to address some of these complications. The two primary complications that the proposed design seeks to address are thrombosis and restenosis. As for the former, typical implanted stents trigger a remodeling of neighboring tissue. The outward radial force of the stent upon the arterial wall can cause irritation and

initiate thrombosis [20]. Thrombosis is often triggered by the disruption of plaques within the affected arteries [21]. New stent technologies ought to be designed to counter these causes of thrombosis in order to address the issue at its most common sources. Advances in drug-eluting stents (DES) and other modern stent technologies have made very late stent thrombosis a rare occurrence [22]. However, instances of thrombosis are still common in the period of recovery following the stenting procedure, which continues to make this condition a point of concern for biomedical engineers.

In addition to thrombosis, the medical condition of restenosis is a substantial consideration in the field of stenting. Restenosis is the most common biological complication associated with implanted stents [23]. Stent implantation has a high rate of restenosis that often leads to repeat vascularization by percutaneous or surgical methods, increasing both medical risks and cost of treatment [24]. As a result, in-stent restenosis (ISR) has been found to occur in 20-50% of stented blood vessels [25]. With such a high rate of this medical condition, it is extremely important for advanced stenting technologies to be developed that can reduce the likelihood of collapse or fracture during normal operation.

Vascular injuries caused by interaction between the stent and the arterial tissue serve as the stimulus for the development of intimal hyperplasia and restenosis [26]. Vascular injuries caused by the implantation of coronary stents has been found to determine the intensity of restenosis in patients [27] [28] [29]. There are several key factors that contribute to the risk and severity of in-stent restenosis (ISR). In general, restenosis is closely linked with the design of implanted stents [30] [31]. Stent platform design drives performance in clinical trials [32]. Consequently, the design of advanced implantable stent

technologies must be crafted to address these factors for the safety of the affected patients.

A proposed solution to these problems is the use of shape memory alloys (SMAs) to create stents that can be placed with greater precision than typical coronary stents, SMAs have the ability to undergo plastic deformation and return to their original tempered shape when heated, potentially allowing for body heat to return deformed SMAs to their original form [33]. Some SMAs, like Flexinol, can also change their shape when appropriate electrical currents are run through their length, serving as actuation for lightweight robotics without need for bulky motors or applied forces to contract or expand the material [34]. In contemporary research, modern SMA stents are constructed with nitinol, which allows for the heat of the patient's body to expand the stent to the desired configuration [35] [36]. Current papers on the use of shape memory alloys employ use of their deformations as a source of linear actuation, which is predicated upon linear expansion and contraction, a chief concern of my thesis. As Flexinol is a variant of nitinol specifically engineered to enhance its contraction properties, it is an ideal candidate for use in SMA stents [37]. As a result, this research examines the behavior of Flexinol and applies the acquired knowledge to the biomedical application of arterial stent technology.

A doctoral student at Carlton University produced a dissertation on the behavior of nickel-titanium shape memory alloys that will prove helpful in this thesis [38]. His research included mathematical modeling of nitinol and Flexinol wires and serves as the foundation in this thesis to utilize his one-dimensional models in order to develop three-dimensional mathematical models for tubular mesh stents comprised of such wires. Further testing and mathematical modeling of Flexinol wires provide the basis for controlling Flexinol contraction via applied electrical current [39].

The Flexinol composition of the stents developed during the research for this thesis will allow for them to be deformed into shapes appropriate for placement within an artery via applied electrical current, and then opened to allow for proper blood flow. Whereas typical medical stents require compression and tension to contract and expand the mesh tubing during placement, the stents developed in this project will have the ability to be actuated to contract via electrical current and expanded to their original shape during placement by the heat of the patient's body in combination with stopping the electrical current to the stent [40]. In this thesis, it is hypothesized that stents engineered with Flexinol mesh will be a safe alternative to modern stents that will allow for easier placement and replacement than those currently in use. It will also exhibit superior controllability. The addition of a control system will allow for doctors to contract the stents to appropriate dimensions for insertion into a wide range of artery diameters, which varies from patient to patient. Control will also allow for precise expansion of the stent as it is placed in an artery, as well as grant doctors the ability to easily contract the stent if it is initially placed in an improper manner, reducing the likelihood of improperly placed stents and medical emergencies as a result of such.

In clinical trials, the implantation of metal stents showed an immediate advantage to plain balloon-angioplasty, leading to a drastic reduction in occurrences of restenosis [9] [15]. This is the result of the stent exerting a radial force upon the tunica interna to hold the vessel open after deployment. The stents developed in this thesis must be analyzed to determine the effects of stress upon the implanted device, and thus, the surrounding artery.

Coronary artery stents are typically divided into three primary groups, including bare metal stents (BMS), drug-eluting stents (DES), and bioresorbable stents (BRS), the

latter of which is further divided into drug-eluting and non-drug-eluting varieties. Permanent placement of BMS has been shown to reduce the likelihood of restenosis in patients after undergoing a balloon angioplasty to reopen the blocked artery [7].

In recent decades, biomedical engineers developed bioresorbable stents that degrade in the blood vessel over time and get absorbed into the body [41]. Biodegradable stents support the blood vessel as it strengthens and allow the artery to return to relative normalcy as they are absorbed by the human body [41] [42]. Stents with biodegradable drug-eluting polymer coatings act as DES in early stages, and later as BMS when the polymer coating is absorbed by the body [43]. DES typically provide greater advantages and increased safety over BMS [43]. Because DES are usually designed upon an existing BMS platform, it makes sense to examine the use of new BMS designs in order to serve as the basis for the advancement of DES. While there are encouraging studies demonstrating the benefits of stents coated with biodegradable polymers and the safety of such, future work must involve long-term effects of their use in the patients with stented arteries and is outside of the scope of this work [44] [45].

Modern “second generation” DES stents are often made of alloys to increase their strength, thus reducing the overall thickness of the struts [43]. By designing with less material, the stents are considered to have better biocompatibility than stents with a greater quantity of non-biological material. However, this increases the stress concentration in the stent struts, making them more prone to failure. These types of stents have become the most common DES stents on the global market, replacing first-generation DES and BMS technologies in many instances [46]. Despite this, many safety concerns surround second-generation DES [43]. While drug-eluting stents have been shown to reduce the rate of in-

stent restenosis, late stent thrombosis is still a major concern with contemporary technologies of this type [47]. In either case, BMS also serve as the platform for DES, so it is important to develop a functional and robust BMS design in order to facilitate further development of the stent technology. Any advances in DES technology are dependent upon progress in BMS technologies. With the number of cases of heart disease increasing, the demand for advanced stenting technology is expected to increase [48].

1.2 Research Objective

The research objective is to design a coronary artery stent that is self-expandable and exhibits characteristics that suggest that its use is likely to improve patient outcomes for those that must undergo emergency revascularization procedures. The goal is to develop an innovative approach to arterial stenting and to verify that approach.

1.3 Research Question

What are the governing characteristics of the shape memory alloy Flexinol and how can we effectively utilize Flexinol shape memory alloy as a bare-metal stenting platform in such a way as to reduce some of the common complications associated with modern stenting technologies?

1.4 Working Hypothesis

With the development of constitutive equations to predict the electrothermal contraction behavior of the SMA Flexinol, it is possible to develop a Flexinol BMS stenting platform that can renormalize blood flow in stenosed arteries while reducing the stress concentration in the stent itself, thus reducing the likelihood of medical complications resulting from the implantation of such devices.

1.5 Tasks

This thesis includes the completion of a series of important tasks to achieve the research objective.

- Task 1: Develop a universal mathematical model for the thermal expansion behavior of typical metal alloys
- Task 2: Develop a specific mathematical model for the behavior of the SMA Flexinol
- Task 3: Conduct experiments to verify the validity of the mathematical modeling for the SMA wire
- Task 4: Design a closed cell stent utilizing Flexinol as the material
- Task 5: Analyze stress concentrations in the stent via FEA simulations of stent interaction with the arterial wall
- Task 6: Conduct blood flow simulations to observe the effects of the implanted stent design and validate the proposed stent as a solution to stenosed arteries

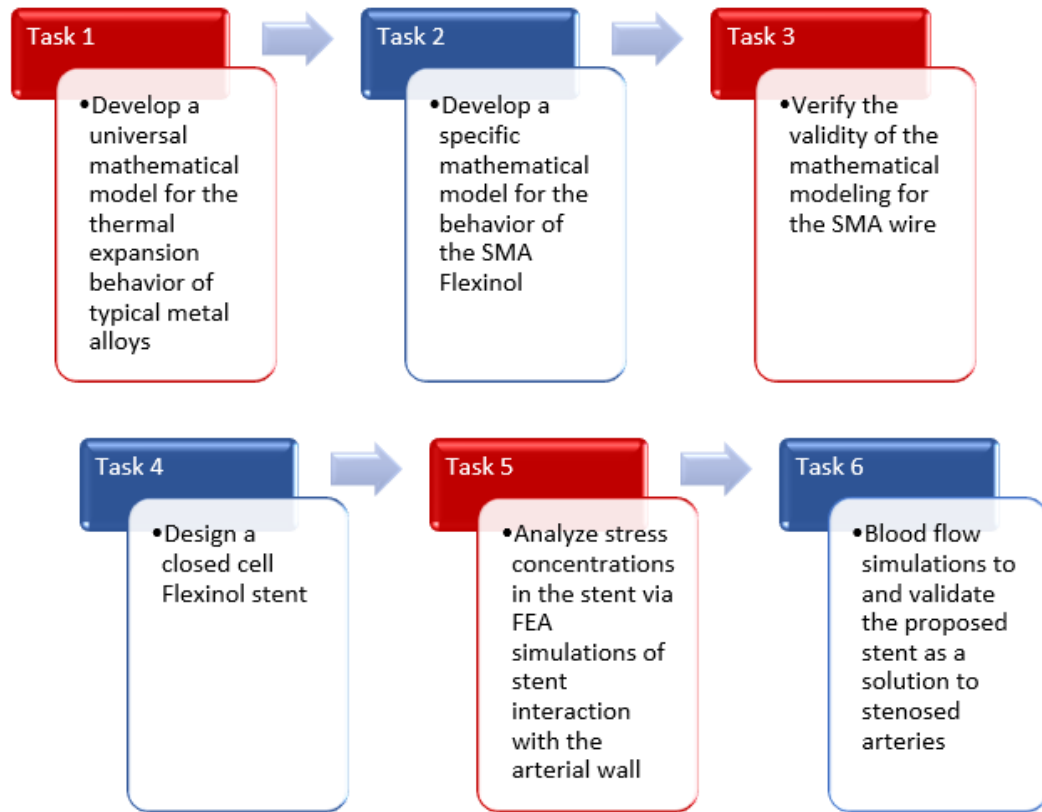


Figure 1. Process workflow of tasks.

Figure 1 depicts the process workflow of the tasks required to complete the research within the scope of this thesis. The completion of such tasks constitutes the attainment of the research goals associated with this work.

1.6 Organization of Thesis

This thesis is divided into a number of chapters. Chapter 1 is an introduction to the issue of coronary artery disease, its characteristics and its treatment. In particular, the revascularization method of stenting coronary arteries is discussed, establishing the background for this thesis. Chapter 2 presents the properties of the shape-memory alloy Flexinol, including the development of mathematical models to describe the behavior of such when subjected to an electrical current. Chapter 3 applies the mathematical models to create a bare-metal stent comprised of Flexinol and presents an innovative method of stent deployment. Chapter 4 examines the flow of blood through the proposed Flexinol stent with computational fluid dynamics methods. Finally, conclusions and recommendations for future research are presented in Chapter 5.

Chapter 2

Behavior of Flexinol Wire

2.1 Introduction

This thesis seeks to develop and test a framework for understanding and predicting the electro-mechanical behavior of the SMA Flexinol, so that the material may be utilized for biomedical applications, such as self-expanding stent technologies. In order to implement Flexinol in such applications, one must first understand the physical processes governing shape-memory effects in typical SMAs. From here, it is important to differentiate the properties of Flexinol from those of other SMAs, such as Nitinol. Understanding these concepts will provide the basis for developing a method of controlling the behavior of Flexinol in stenting technologies.

It is of tremendous importance to derive the mathematical equations that govern the behavior of Flexinol wire in order to truly comprehend the practical behavior of this material. First, a general mathematical formulation for metal alloys should be developed and then specified to be applicable to SMAs, particularly Flexinol. Because SMAs undergo crystalline phase transformations that drastically alter the resistance of the material while an electrical current flows through a wire comprised of the material, it is important that mathematical models account for the variable resistance. Such advancement of knowledge in the field of SMAs will serve as a necessary basis for establishing control mechanisms for SMA wires.

Experimental verification of said mathematical models is essential to ensure that the theoretical research presented in this chapter can be applied to practical scenarios. This chapter provides the indispensable research that allows for the design and development of Flexinol stenting technologies, as well as the basis for future advances in the use of controllable SMAs for applications in the biomedical field and beyond.

2.2 Literature Review

Shape-memory alloys (SMAs), such as Nitinol, are materials that can undergo plastic deformation and return to their undeformed shape when heated. SMAs undergo a crystal transition between a martensite phase and an austenite phase as the material temperature increases [49]. SMAs may be tempered into a particular shape or configuration in the martensite phase prior to being mechanically deformed into a separate shape. This plastic deformation causes a phase change in the crystalline structure of the material. When the material is heated, the material undergoes a reversal of this phase change, causing a return to the originally tempered shape or configuration. This process is known as the “shape-memory effect” [50].

When subjected to low temperature conditions, SMAs display a small elastic modulus and can be deformed rather easily [49]. Some SMAs can also be antagonized to alter their shape when electrical currents are applied, causing appreciable contraction and expansion that can be captured for mechanical work [34]. Whereas most materials expand when heated, these SMAs can be tempered to contract when an electrical current is applied and return to their original shape after the current is ceased. These SMAs are often

fashioned into wires that can be used as mechanical actuators when a current is applied [51]. It is this electromechanical behavior that is of much interest to this research. As an SMA changes its shape, the metallographic transformations from the martensite to austenite phases cause a significant change in the electrical resistance of the material, this implies that the strain of the wire can be controlled via a variable electrical input [49] [52].

One such SMA is Flexinol, a variant of nitinol, which is the most widely used SMA. Flexinol is an alloy comprised primarily of nickel and titanium that was designed to exhibit optimized characteristics for actuation, including an extensive work life, high repeatability, and strength for shape recovery [37]. Nitinol has been extensively studied in scientific literature in order to understand its behavior, but Flexinol has not been examined to the same extent. It is known that nickel and titanium-based shape memory alloys can exhibit a recoverable strain of up to 8%, but it is recommended that the strain not exceed 4% of the overall length of the wire to ensure a high number of usage cycles [34]. In a biomedical application, the strain of the wires does not have to be recovered, allowing for the use of increased strain.

SMA actuators have been experimentally shown to be accurately controlled by position and force feedback when the properties of the SMA are known [53] [54]. Such control requires mathematical models that consider the material properties, the mechanics of the system, and the thermal properties of the significant components involved in the machine. As expected, the behavior of SMA wire can be very non-linear [38]. Because of the great difficulty in modeling the behavior of a particular SMA for a given mechanical system, SMA actuators are often used without accurate feedback control systems and many applications require extensive trial and error in order to develop a working model [55].

This thesis includes the development of mathematical equations that predict the behavior of Flexinol wires in one-, two-, or three-dimensional space.

The complex dependence of the resistance of the SMA wire on temperature and stress is not well understood and limits its applicability as a feedback signal [39]. It has been found that the resistivity of SMA wires is appreciably affected by the load stress within the wire [56]. As such, mathematical models must be developed that include the stress as a major variable. Some preliminary work has been done in this area, providing a basis for the project presented in this paper [38] [39]. However, much of the research available is incomplete and piecemeal, requiring extensive mathematical development to yield practical value to this project. Further, there is a lack of uniformity in the quality and physical properties of the material among samples produced by the manufacturer, causing studies to use an assumed average for several material properties [38].

However, there are several useful findings in regard to the control of Flexinol. While the Flexinol will flex approximately 4% of its total length when used for these applications, a control program would have an output error less than 4% of that length, or less than 0.16% of the overall length of the wire [38]. Because the stenting technologies presented in this thesis are incredibly small, having the ability to precisely control the contraction of the Flexinol wire mesh that comprised these stents is of paramount importance. With such a small output error, Flexinol can confidently be used to achieve the aims of this thesis. As such, this research provides the basis for further study and development of the use of electrically powered SMA wires to serve as the wire mesh that comprises the platform for both BMS and DES technologies.

SMA actuation provides a high strength to weight ratio and allows for the miniaturization of robotic systems [57]. Such implementation eliminates the need for bulky servo motors that hinder the miniaturization of robotic prototypes. This is especially useful in applications that utilize wire or mesh material configurations, as it allows for the wire itself to serve as the actuation mechanism. This means that the placement and utilization of the stent can be self-contained in a single mechanism, rather than a complex system with many possible sources of error.

The design developed in this study utilizes the SMA wire as the actuation mechanism to expand and contract the proposed stent design. This is somewhat similar to typical cable-driven actuation in miniature robotic applications, including robotic hands. The issue with the use of SMA wire as actuating tendons is that they are typically restricted to external use, rather than full integration of the SMA in the fashion of a tendon in human biology [34]. By incorporating the actuation mechanism into the device, it allows for the stent to be designed as a compact system.

2.3 Mathematical Formulation of the Resistive Behavior of Standard Metals

In order to understand the resistive behavior of Flexinol, it is important to develop the equations that govern the resistance of typical materials that do not exhibit the shape-memory effect. In doing so, I was compelled to simplify the resistance model to hold the resistivity constant, but account for the variation in the length and cross-sectional area of the wire as it expands and contracts. This becomes the basis for a separate model of the

contraction of Flexinol wire that could be generalized to any material, rather than just SMAs.

$$R = \rho \frac{L}{A} \quad (1)$$

where R is the resistance of the wire, ρ is the resistivity of the wire, which is considered to be a material constant, L is the initial length, and A is the initial area of the wire.

Using Poisson's ratio to determine how the area changes with respect to the changing length, I used the following Poisson's equation.

$$\nu = -\frac{\Delta d}{d_i} \frac{L}{\Delta L} \quad (2)$$

where ν denotes the Poisson's ratio of the material, Δd is the change in diameter of the wire, d_i is the initial diameter of the wire, and ΔL is the change in length of the wire. For purposes of this project, ΔL is equivalent to δ_h .

I utilized the equation for the cross-sectional area of the wire (Equation 3) in order to relate the resistance of the wire to the variation of the wire length and diameter.

$$A = \frac{\pi(d_i - \Delta d)^2}{4} \quad (3)$$

$$R = \frac{4\rho(L + \Delta L)}{\pi\left[d_i\left(1 - v\frac{\Delta L}{L}\right)\right]^2} \quad (4)$$

This allowed me to construct the following equation for the displacement due to the contraction of the wire.

$$\delta_h = a_h \frac{4\rho(L + \Delta L)}{\pi\left[d_i\left(1 - v\frac{\Delta L}{L}\right)\right]^2} + b_h \quad (5)$$

Equating ΔL and δ_h and arranging into a third-order polynomial, I obtained the full equation for the displacement of an end of the wire when subjected to an electrical current. The solution to which may be found using the formula for the roots of a third-degree polynomial.

$$\frac{\pi d_i^2 v^2}{L^2} \delta_h^3 + \frac{d_i^2 v}{L} \left(-2\pi - b_h \frac{v}{L}\right) \delta_h^2 + \left(\pi d_i^2 - 4a_h \rho + 2b_h d_i^2 \frac{v}{L}\right) \delta_h + (-4a_h \rho L - b_h d_i^2) = 0 \quad (6)$$

For the control of the contraction of Flexinol, I used Ohm's Law to incorporate the varying resistance of the Flexinol wire.

$$V = IR \quad (7)$$

Plugging equations 1 and 3 into this, I obtained the following equation for the control of the resistance for purposes of metallic wire actuation. This method can be used to control small contractions of typical metallic materials, piezoelectric materials, and even SMAs, with corrections for resistance.

$$R = \frac{L^2}{v^2} \left[-\frac{2I\rho}{v\pi d_i^2} - \frac{v}{L} \pm \frac{2}{d_i} \sqrt{\frac{I^2 \rho^2}{v^2 \pi^2 d_i^2} + \frac{Iv\rho(v+1)}{v\pi L}} \right] \quad (8)$$

Which was then plugged into Equation 5 to obtain the complete equation for the control of the system and expressed more simply through the use of defined constants.

$$\delta_h = \alpha \left[-\omega\beta - \frac{1}{\sqrt{\alpha}} \pm \gamma \sqrt{\omega^2 \varepsilon + \omega\theta} \right] a_h + b_h \quad (9)$$

where the constants are defined by known quantities, shown below.

$$\alpha = \frac{L^2}{v^2} \quad (10)$$

$$\beta = \frac{2\rho}{\pi d_i^2} \quad (11)$$

$$\gamma = \frac{2}{d_i} \quad (12)$$

$$\varepsilon = \frac{\rho^2}{\pi^2 d_i^2} \quad (13)$$

$$\theta = \frac{v\rho(v+1)}{\pi L} \quad (14)$$

The constants a_h and b_h are experimentally determined and can be compound in nature. In order to derive this, it is imperative that actual material be tested. These constants are derived from experimental data for Flexinol SMA in the previous section, based on experimental data relating the constants to the stress within the wire.

As the actuation of the wire is dependent upon the ratio of electrical current and applied voltage, it is convenient to also define the electrical control variable to simplify the control equation. The control variable ω can be adjusted by either varying the voltage across the wire or the electrical current through the wire.

$$\omega = \frac{I}{V} \quad (15)$$

The following Table includes relevant values provided by the manufacturer of the Flexinol wire that proved invaluable in the modeling of the behavior of the such wires. This is predicated upon the particular wire sample used in the experiments within this thesis. These values assist in the validation of the mathematical model developed in this section. The resistivity value included within the Table is the average between the manufacturer's provided values for the martensite and austenite phases [58].

Table 1. Average material properties of Flexinol wire sample.

Constant	Value
v	0.33
d_i	125 micrometers
ρ	90 micro-ohms * cm

Using a sample of Flexinol wire of 20 cm in length, I tabulated sample values for each of the constants in equations 10-14. These constants allow for a greater understanding of the behavior of the Flexinol wire when subjected to an operating current. Numerical values for these constants are necessary for the completion of the control equation and its subsequent verification. These constants are displayed in Table 2.

Table 2. Numerical values for Flexinol constants.

Constant	Value
α	0.4444 m^2
β	$3666.9 \frac{\Omega}{\text{m}}$
γ	$16000 \frac{1}{\text{m}}$
ε	$0.0525 \Omega^2$
θ	0.00005586Ω

I used the manufacture-provided maximum pull force value of 2.187 Newtons and Equation 6 to predict the maximum deformation in the wire. Utilizing Matlab to solve for the roots of the equation, I found that the theoretical maximum deformation in the 20 cm wire is equivalent to 5.05 cm, or 25.3% of the length of the wire, which is much higher than the 8% maximum recoverable strain quoted in the literature. This suggested that when a sufficiently large current simultaneously with a large load, unrecoverable strain deformations occur that permanently damage the wire. With this in mind, I designed the Flexinol stent to avoid excessive strain due to unnecessary loading conditions.

2.4 Mathematical Formulation of the Resistive Behavior of Flexinol

For this thesis, I was able to utilize research on the behavior of Flexinol wires and incorporate the information into a viable mathematical model to represent its behavior when subjected to variations in electrical current. The contraction of Flexinol wires such

as those intended for use in SMA stent applications was found to be modeled by the following equation 16 [38]. This relationship accounts for the stress in the wire, which made it an ideal basis for the mathematical model of the behavior of Flexinol when subjected to an applied electrical current.

$$\delta_h = a_h R + b_h \quad (16)$$

where R is the resistance value, determined by a function of the input voltage and current. The subscripts refer to the heating of the wire, as there is a parallel equation for the cooling phase of the Flexinol wire. For the purposes of this thesis, the heating equations are the most important, as they rapid response of the SMA material when a current is applied. One can delineate the heating and cooling thermal phases as the “active” and “passive” thermal phases of the material expansion and contraction. The variables a_h and b_h are functions of the stress applied to the wire and obtained via equations 17 and 18. Values of the coefficients were determined by measuring the heating slope and intercept of the equation with respect to a variety of applied stresses and tabulating the data to generate a best-fit polynomial equation.

$$a_h = 0.000002\sigma^2 - 0.0009\sigma + 0.6875 \quad (17)$$

$$b_h = -0.00005\sigma^2 + 0.0203\sigma - 11.927 \quad (18)$$

For these equations, σ denotes the stress in the wire, in terms of MPa. The constant values for Equation 17 are in mm/ Ω and Equation 18 are in mm. In equation 16, the a_h term relates the stress and the resistance of the wire, and the b_h term describes the deformation of the material due to applied stress without an electrical current.

Because Flexinol is a shape-memory alloy, I am compelled to consider the variation in electrical resistivity between the martensite and austenite phases. The total resistance of the wire is a function of the fraction of the material in each phase and their associated resistances [39]. This total resistance changes significantly as the material undergoes a partial or complete phase transformation via heating processes. The equation representing the total electrical resistance of Flexinol wire is displayed as equation 19.

$$R_{tot} = R_M \xi_M + R_A \xi_A \quad (19)$$

In which R_M is the resistance of the wire in the martensite phase, R_A is the resistance of the wire in the austenite phase, ξ_M is the phase fraction of martensite, and ξ_A is the phase fraction of austenite. The resistances of the wire in each phase are functions of the temperature and applied stress.

$$R_M = R_{0M} + (T - T_{0M}) \frac{\partial R_M}{\partial T} + \sigma \frac{\partial R_M}{\partial \sigma} \quad (20)$$

$$R_A = R_{0A} + (T - T_{0A}) \frac{\partial R_A}{\partial T} + \sigma \frac{\partial R_A}{\partial \sigma} \quad (21)$$

The parameters in these equations are presented in Table 3. Experimentally determined values for each of these parameters with a Flexinol wire with a diameter of 250 micrometers are presented in Table 4.

Table 3. Parameters of Flexinol phase change.

Parameter	Description of Parameter
R_{0M}	Nominal resistance in martensite phase
R_{0A}	Nominal resistance in austenite phase
T_{0M}	Nominal temperature for martensite phase
T_{0A}	Nominal temperature for austenite phase
$\frac{\partial R_M}{\partial T}$	Temperature dependence of resistance in martensite phase
$\frac{\partial R_A}{\partial T}$	Temperature dependence of resistance in austenite phase
$\frac{\partial R_M}{\partial \sigma}$	Stress dependence of resistance in martensite phase
$\frac{\partial R_A}{\partial \sigma}$	Stress dependence of resistance in austenite phase

While this work is invaluable in understanding the resistance behavior of Flexinol wires, there lacks a significant study into the phase fractions of the two primary phases. As

shown in Figure 2, the total resistance can lie anywhere between the two curves, potentially leading to large errors in calculating the resistance at a given temperature and stress and urging further research into the resistive behavior of Flexinol wire as the material undergoes phase transformations.

Table 4. Numerical values for Flexinol phase change parameters.

Parameter	Experimentally Measured Value
R_{0M}	5.08 Ω
R_{0A}	4.82 Ω
T_{0M}	0 $^{\circ}\text{C}$
T_{0A}	225 $^{\circ}\text{C}$
$\frac{\partial R_M}{\partial T}$	6.14 $\frac{\text{m}\Omega}{^{\circ}\text{C}}$
$\frac{\partial R_A}{\partial T}$	0.802 $\frac{\text{m}\Omega}{^{\circ}\text{C}}$
$\frac{\partial R_M}{\partial \sigma}$	0.821 $\frac{\text{m}\Omega}{\text{MPa}}$
$\frac{\partial R_A}{\partial \sigma}$	0.390 $\frac{\text{m}\Omega}{\text{MPa}}$

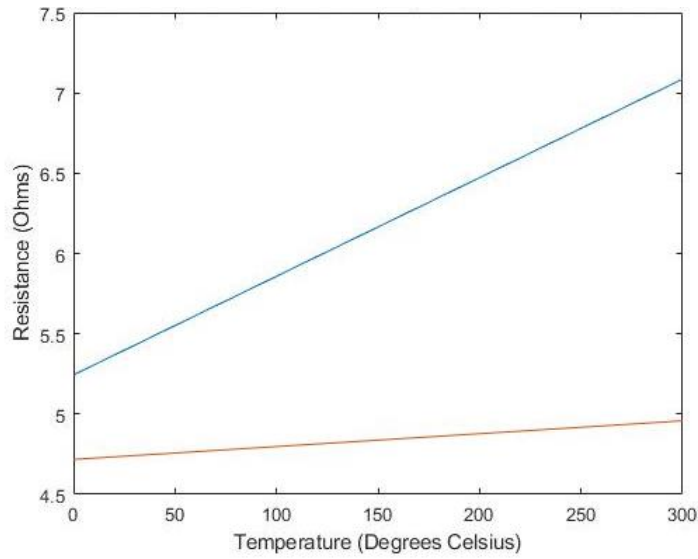


Figure 2. Plot of Resistance Curves for Martensite (Blue) and Austenite (Red) Phases.

In order to obtain a useful model from this information, I was compelled to provide an assumption as to the transformative behavior of the Flexinol between the martensite and austenite phases. For purposes of comparison between the mathematical predication and later experimental results, it was assumed that the resistance itself could be approximated as linear behavior in order to generate a complete picture of the resistance. In this effort, I assumed that the Flexinol wire is entirely in an austenite phase at the nominal temperature for this phase, and that the wire is entirely in the martensite phase at the nominal temperature for that phase, which yielded equations 22 and 23 for the phase fractions of each phase. Having inserted these into equation 19, I was able to model the predicted resistance of the Flexinol wire, as shown in Figure 3.

$$\xi_A = \frac{1}{225}T + 0 \quad (22)$$

$$\xi_M = -\frac{1}{225}T + 1 \quad (23)$$

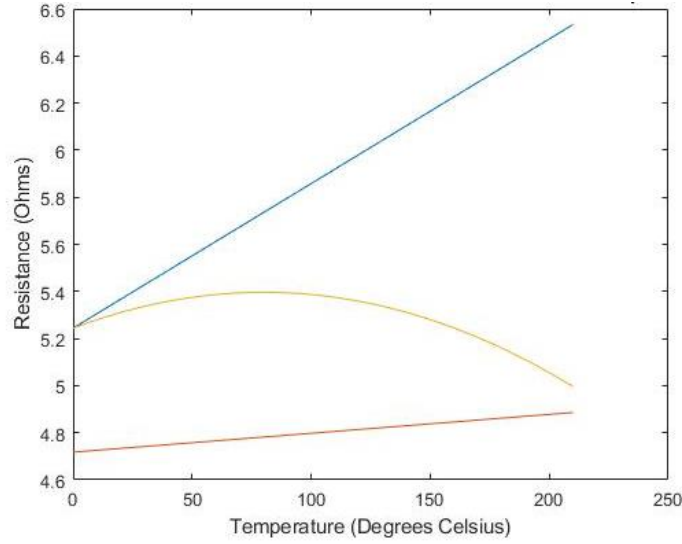


Figure 3. Plot of Resistance Curves with Linear Transformation Assumption.

From this, it is shown that the behavior of Flexinol wire is physically bounded by the upper (martensite) and lower (austenite) limits. This should remain true when variations in the composition of the Flexinol are accounted, such as slight variations in the ratio of nickel to titanium within the alloy. In all of these cases, the thermal expansion behavior should fall within these limits. It is also shown that as the temperature of the material increases, the phase change from martensite to austenite alters the internal resistance of the material to a significant degree. With the boundary equations known, the maximum and

minimum material reactions are known. This aids in the generation of a more complete picture of the material's overall thermal behavior.

Knowing how the material reacts to variations in temperature, as well as how the internal resistance of the Flexinol wire changes with such variations, it is possible to relate the internal temperature to the contraction of the wire. Equation 24 displays the various equations for determining the electrical power input into the wire.

$$P = IV = I^2R = \frac{V^2}{R} \quad (24)$$

This approximates the power that is converted into thermal energy that heats the Flexinol material as the electrical current flows through. This is the basis for joule heating that dictates the internal temperature of the wire and governs the internal resistance value. With a manufacturer-provided heat capacity of 0.32 J/gC, equations 25 and 26 were formulated to represent the change in temperature as a result of joule heating.

$$\Delta T = 0.32 * I^2R \quad (25)$$

$$\Delta T = 0.32 \frac{V^2}{R} \quad (26)$$

For simplicity, equations 25 and 26 can be combined as equation 27.

$$\Delta T = 0.32 * P \quad (27)$$

This equation forms the second half of the interdependent relationship between the temperature and resistance of the Flexinol wire. As the temperature changes, the crystalline structure of the SMA is altered, which changes the resistance through the material. This change in resistance drives the rate of joule heating of the material, and thus, the rate at which the temperature changes. It is important to understand this interdependent relationship for the purposes of controlling and predicting the behavior of the material when utilized as the basis for stenting platforms.

If convection cooling is factored into the equation, such as in a real-world scenario, the internal heating of the material will compete with the tendency for that heat to escape into the surrounding air. This means that the wire will not heat infinitely but will reach a thermal equilibrium as the energy input matches the energy loss to the surroundings. It is intuitive that higher wire resistances correspond to thermal equilibriums at higher temperatures.

2.5 Experimental verification

Flexinol wire samples of various diameters were obtained for use in verifying experiments. Connecting these samples in a series circuit and generating a current using an Arduino Uno microcontroller caused the electrothermal contraction of these wires and provided insights into the resistance behavior of Flexinol. The experimental setup is displayed in Figure 4, and shows the Arduino configured to run a current through the wire with an operating voltage of 5 volts. As shown, one end of the Flexinol wire was secured to the Table to ensure that strain measurements were accurately conducted. The other end of the wire was loosely attached to a wire that was then connected to the Arduino breadboard, which allowed the Flexinol wire to experience measurable contraction. During the experiments, a digital multimeter was utilized to measure the electrical resistance across the Flexinol wire and the strain was measured with a ruler and caliper.

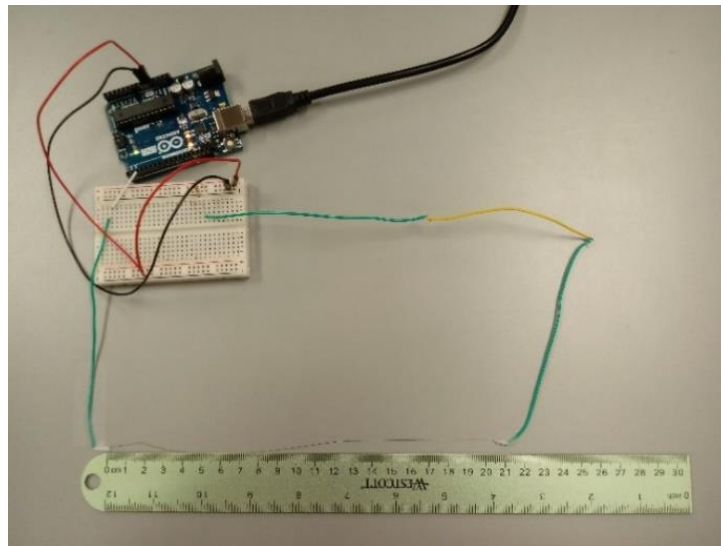


Figure 4. Experimental Setup.

In these experiments, low-temperature Flexinol wires of various diameters were used to complete a simple circuit, causing the wires to contract as the movement of electrons through the wire caused the material to heat. This exemplified a conversion of energy from electrical to thermal and produced a thermomechanical response of the material. Several variables were recorded, including the required time for the wire to contract by the manufacturer's recommended value of 4%. The information obtained by tests conducted at an input voltage of 5 volts and 3.3 volts yielded the relationship between the wire diameter and the current flowing through the Flexinol material at a given voltage. This is displayed in Figure 5. From this, one can derive the resistance of each wire to predict their behavior when subjected to various electrical conditions.

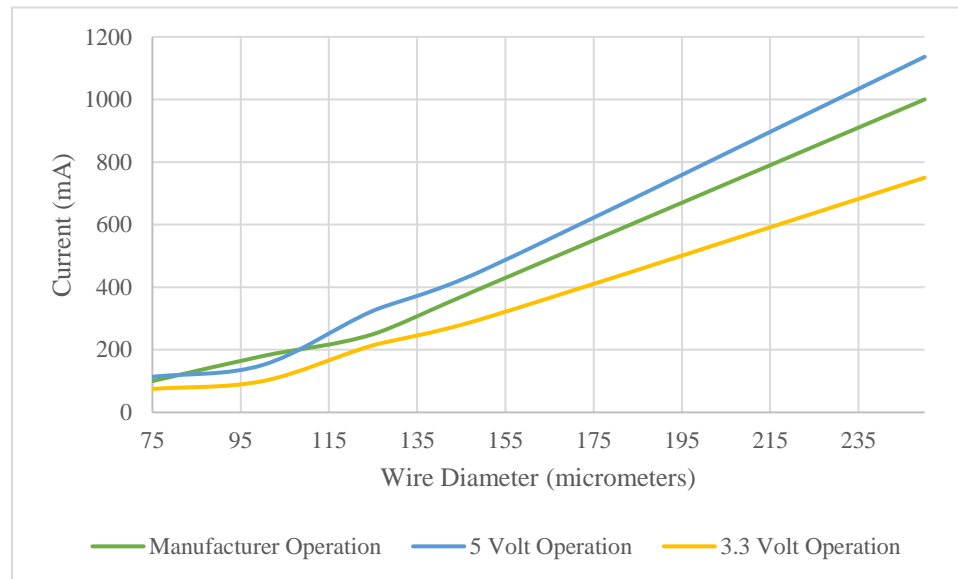


Figure 5. Current vs. wire diameter for various operating conditions.

From these experiments, it is initially difficult to discern whether the governing equations derived earlier in this thesis hold true. However, an analysis of the data set reveals some interesting features that aid in the verification of the governing equations. As displayed in Figure 4, the wires at lower diameters encounter variations in their behavior. This can be attributed to the phase change from martensite to austenite and the associated alteration to the material's resistance. After the phase change is complete, the curves on the graph become quasi-linear, suggesting uniformity after the phase change. It is clear that the antagonization of the phase change can be controlled by the variable of voltage across the wire.

As shown, higher voltage operation corresponds to higher current through the wire. This causes the material to heat at a faster rate, which allows the material to contract in a reduced period of time. This is evidenced by experimental data obtained by measuring the displacement of Flexinol wires of various thicknesses and the resistance across the material as it was heated with an electrical current. For the sake of simplicity, the 150-micrometer diameter Flexinol wire test is shown below, as it is characteristic of the behavior of the Flexinol wire behavior throughout the range of sizes. The results of this test are shown in Figure 6.

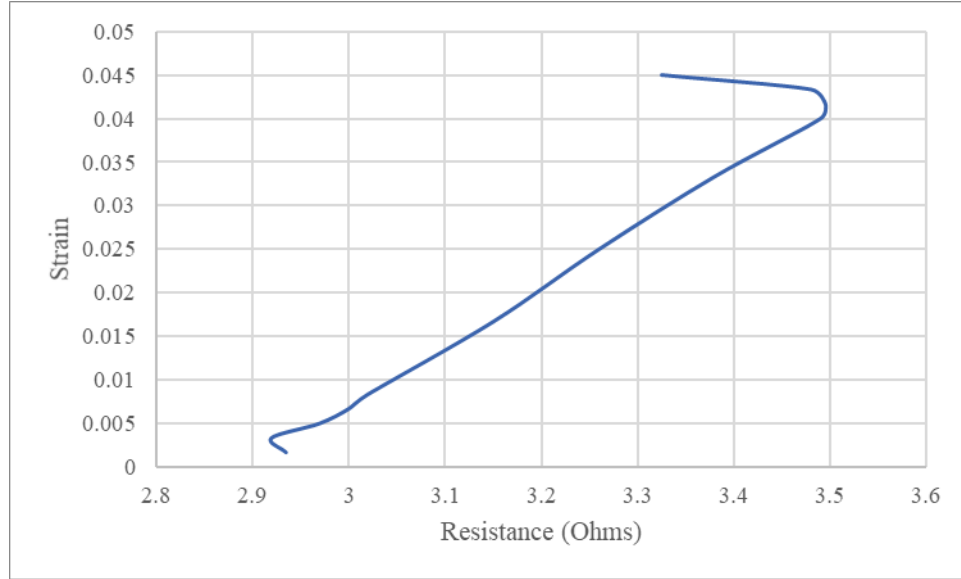


Figure 6. Resistance versus strain in Flexinol wire sample.

With the data obtained from these experiments, it is possible to solve for the average resistance in each wire diameter, which will provide a near verification of the equations derived in sections 2.3 and 2.4. The deviations at the top and bottom of the curve are associated with the initiation of the phase changes of the Flexinol wire. This occurs at the beginning and end of the curve because it corresponds with the application of higher electrical power that contributes to faster Joule heating. Utilizing the linearized model from equation 16 and solving for the constants from equations 17 and 18, the predicted performance of the wire can be found. This is compared with the experimental results in Figure 7.

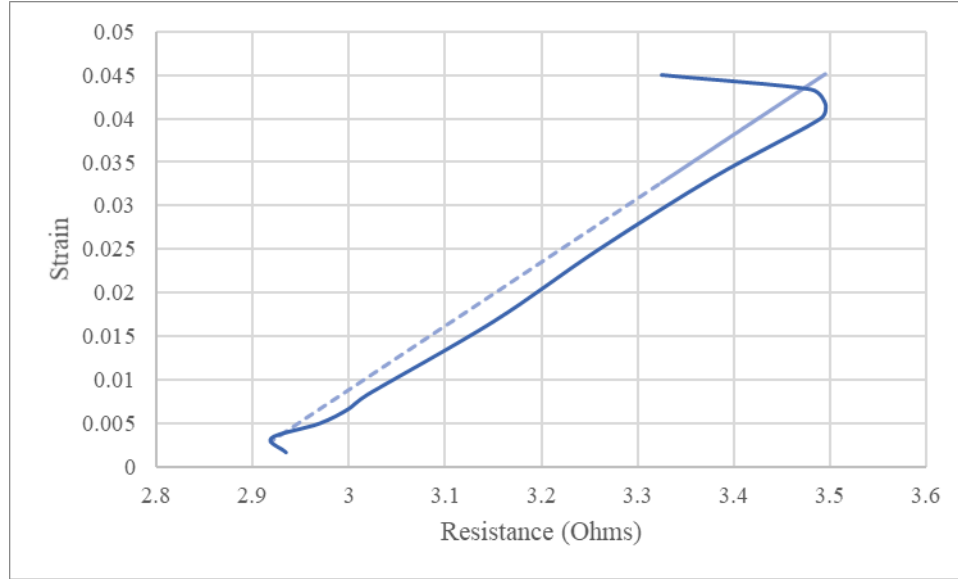


Figure 7. Plot of resistance related to strain. Theoretical response is predicted with the dashed line, experimental data is displayed with a solid line.

As shown in Figure 7, the experimental data follows the linearized constitutive model. The linear portion of the experimental data curve is within 2% of the predicted behavior of the material, confirming that this mathematical model can be used to predict the behavior of Flexinol. It must be noted that the deviations at the top and bottom of the curve are associated with the initiation of the phase change of the Flexinol wire, as in Figure 6. This introduces a degree of nonconformity when compared to the mathematical model. Additionally, the resistance of a physical wire sample is certain to deviate from the predicted case, as shown by the higher resistance seen in the experimental data. This could be corrected by adjusting the third term in equation 16, which governs the constants that are specific to individual Flexinol samples.

Considering the tensile force of less than one newton within the wire, equation 6 was solved for the displacement. As this is a third order polynomial, three possible answers were found. However, two of them were much too large to be considered as a feasible answer to the real-world problem. With this in mind, the value of strain of 5% was selected as the maximum possible displacement. This seems to be consistent with the experimental data shown above, which serves to verify that the complex mathematical model and the experimental data is reliable. This confirmation allows for the prediction of the behavior of Flexinol alloys in sophisticated applications.

2.6 Closure and future work

The governing equations derived in this chapter serve as the basis for predicting the behavior of the SMA Flexinol. Through experimental verification, it is shown that these methods can be used to predict, and thus control, the behavior of this material. Because of this, the research presented offers a clear understanding of the material in question and opens the door to its use in a wide variety of delicate and intricate applications.

It is recommended that the governing equations be tested under a variety of loading and heating conditions in order to determine the effects of external forces and energy transfer on the system. In practical applications, these variables ought to be considered, as they play a role in determining the rate and extent to which the SMA expands or contracts. Future work would involve a series of tests with substantial tensile stress in the wire in order to measure the impact of such on the behavior of the material.

With the research generated within this chapter, it is possible to predict the behavior of Flexinol wire under a variety of loading conditions. As a result, Flexinol wire can be utilized in more sophisticated applications and be controllable via consideration of a variety of input factors, both electrical and mechanical. This thesis serves to present the possible application of Flexinol as a basis for coronary artery stenting platforms. By generalizing the governing equations of the SMA Flexinol, it is possible to control the behavior of a three-dimensional array of Flexinol wires with an electrical input.

Chapter 3

Flexinol Stent as a Self-Expanding Bare Metal Stent

3.1 Introduction

While standard nitinol self-expanding stents have been on the market for a considerable amount of time, there has yet to be significant study into the implementation of Flexinol as a possible stenting platform. This thesis seeks to examine the behavior and biocompatibility of stent designs comprised of this unique material.

Whereas nitinol is antagonized to undergo its phase changes via externally applied heat sources, Flexinol is a specially designed nickel-titanium alloy that can be antagonized by internal heating of the material via electric current. This thesis presents a set of stent configurations that utilize Flexinol as the base material. With the design of coronary stents, it is important to consider all significant factors that impact the performance and safety of the technology.

As with any medical device, there are several potential risks associated with the implantation of contemporary coronary stents. Among these potential risks, stents commonly contribute to late stent thrombosis [59], in-stent restenosis [60], and hypersensitivity reactions [61] [62], among many other potential issues [41] [63]. These risk factors drive the need for advanced coronary stent technologies to reduce the likelihood of complications. Many of these complications are associated with a lack of biocompatibility between the artery and the implanted stent [64].

Stents should be designed, manufactured, and placed in such a manner as to lessen the likelihood or severity of complications over the course of their lifetimes. As such, coronary stents ought to be robust in nature, allowing for a long lifetime of safe use. A significant issue with coronary stents is that many materials will biodegrade over time [41], which can lead to severe complications if the stent was intended to be placed permanently. Therefore, it makes sense to examine the bio-durability of Flexinol to ensure that the material can be used for a long period of time within the human body.

It is also necessary to determine the magnitude and concentration of stresses within the struts of the stent, because excessive residual stress in the implanted stent often leads to the fracturing of the stent strut through a process of local stress corrosion [3]. This is a crucial task for determining the potential success with the use of Flexinol as the platform for the proposed stent designs.

Common stents subject to large residual stresses after deployment are prone to fracturing early in their lifetimes [65]. Even some models of nitinol SMA stents experience a rate of in-vivo fracture near 50% [66]. With such a high rate of stent failures, many coronary stents come coated with medication to relieve the symptoms associated with fractured stents [67].

Nitinol stents tend to exert lower stresses than average compared to other commercially available stent materials. Simulations of various stent designs show that nitinol is consistently one of the least stressed materials utilized in the development of coronary stents [3]. Nitinol allows for large elastic strains, which greatly reduces the risk of stent failure due to high stresses or damage during placement [68]. It is important for

stents to be developed in a fashion that provides a high rate of success with a low likelihood of damage to the surrounding tissue. Nitinol stents have increased the success rate and reduced complications in patients, justifying their use as the framework for additional stent technology development.

Industry standards suggest that nitinol stents should be designed with life cycle of 10 years' worth of fatigue [69]. This corresponds to approximately 380 million cycles. Stents constructed with other SMAs should be designed to meet or exceed this lifespan in order to be a viable option for most patients.

A major difference between the proposed stent design and modern SMA stents is that the proposed stent design is intended to be placed via internal electrical heating, rather than simply relying upon the heat of the patients' bodies. This allows for a more predictable expansion that could improve the chances of proper placement to avoid the complications associated with thrombosis. In order to achieve this, balloon angioplasty is no longer necessary. However, the stent would have to conduct a small electric current in order to heat internally while the body heats the stent externally. While the voltage has little effect upon the physiological response of the body, it is important to ensure that the current is below the perceptible threshold of 1 mA to avoid any complications as a result of current flow [70]. Utilization of the equations for the joule heating (equation 27) and the expansion behavior of the Flexinol material account for this and keep the current within a safe range.

While current SMA stent technologies utilize external joule heating via means of a patient's body heat in order to expand into place, and often still require balloon angioplasty

to ensure that the device fully expands, the proposed Flexinol stent is designed for an innovative method of stent deployment. In such deployment, the stent is heated via both internal and external means, increasing the rate of expansion, as well as the accuracy of placement via controlled deployment.

This process takes a series of steps. The first step is for the attending doctor to select the correct coronary stent for the application. As discussed, this is dependent upon the inner diameter of the patient's artery, the size of the blockage, and other biological factors. The proposed Flexinol stents are designed for use in medium-sized arteries with semi-rigid arterial walls, which may contribute to the type of stent that the physician chooses for the application.

After stent selection, the device must be inserted into the affected artery through surgical means. In order to ensure that the procedure is minimally invasive, the stent ought to be crimped or distorted to reduce its size for the initial stages of placement. For applications where the stent need only be reduced in size by a small amount, this may be achieved by electrically reducing the size of the stent in the method described in chapter 2 of this thesis. As calculated, the SMA wire mesh can contract up to 10% in circumference, which corresponds to a diameter reduction of approximately 3-4%. Such a reduction allows for the stent to return to normal size upon breaking the electrical circuit through the stent.

The second, and recommended, method of placement with the Flexinol stent is to physically deform the stent from its tempered shape. Doing so causes alterations to the crystalline structure within the material. This can be done either at the location of manufacture or in the surgical room in order to be adaptable to the needs of the medical

team when placing the stent within the patient's body. In either case, the diameter, and even the overall shape, of the stent can be altered for ease of insertion into the affected artery. Once placed within the body, the electrical current can be used to return the stent to its originally tempered shape by heating the material internally. Coupled with internal resistance joule heating, the Flexinol stent will receive heat energy from the patient's body through conductive processes. Together, this activates the self-healing nature of the Flexinol SMA and returns the stent to its pre-deformed shape, thus opening the artery for the normal flow of blood after placement.

3.2 Literature Review

Computational studies of nitinol self-expanding stents have been used to investigate the expansion and mechanical behavior involved in their use [71] [72] [73]. This brings to light several health benefits and concerns with modern arterial stenting technology. Ideal stents must have good flexibility, ease of deliverability, the ability to withstand high radial forces, reasonable radio-opacity for x-ray imaging, and good biocompatibility [43].

It is critical that implanted stents be correctly sized to prevent dangerous complications [68]. Stents that are too small for the artery in which they are deployed can migrate or lead to paravalvular damage [74] [75]. Stents that are sized too large can cause damage to the tunica interna and lead to much discomfort [68]. Typical stent sizing requires the diameter of the deployed stent to be greater than that of the surrounding arterial wall by approximately 11% [76].

One of the biggest concerns with the use of stenting technologies is the blood vessel collapsing once again. This is referred to as restenosis and can lead to serious injury or death. It is known that the risk of restenosis is closely correlated with the magnitude and concentration of stresses that develop within the stent after deployment [77]. These stresses are dependent upon a variety of factors, including the deployment pressure and the pulsatile flow of the blood through the stented artery [78] [79] [80] [81]. Excessive stresses caused by a combination of these factors often leads to fracturing of the stent itself and the wall of the artery collapsing inward to further block the flow of blood.

Displacement of built-up plaque and the elastic force of the arterial wall can exert a pressure of up to 0.95 MPa upon the deployed stent [82]. As a result, the rated burst pressure of most stents is approximately 1.6-1.7 MPa [3]. This leaves a typical factor of safety near 1.7-1.8 for most commercially available stent technologies. Even still, many stent designs fail at a much lower stress of 260-190 kPa [68]. Thus, the reduction of stress concentration within the stent structure is paramount to avoiding critical failures.

Due to high stress concentrations at the links between stent struts, these locations are more prone to crack under the pressure of the arterial wall over time [3]. It logically follows that stent failure is closely tied to the thickness and length of the struts [83]. Variations in stent design correlate with different rates of ISR [84] [85]. Therefore, the design of the stent structure is a key to controlling the rate of ISR in patients with implanted stents [77]. Interestingly, trials suggest that thinner struts produce lower rates of ISR [32]. It has been postulated that thinner struts reduce inflammation and neointimal hyperplasia, causing a reduction in the cases of restenosis with the use of such technologies [86] [87].

Thin struts also allow for greater flexibility and low-pressure deployment, reducing the difficulty of the procedure as a whole [88].

The most common material used for bare-metal stents is 316L stainless steel, which is strong and resistant to corrosion [89]. The low density of this material can make it difficult to detect in X-ray imaging [90]. Stainless steel releases heavy-metal ions that can initiate an inflammatory and immune system response, causing in-stent restenosis and neointimal hyperplasia [62].

Stainless steel stents typically have a strut thickness greater than 130 micrometers and have been tested in multiple trials to examine the likelihood of strut failure. [91]. Unfortunately, biomedical engineers have yet to develop a perfect stent, and all stent designs on the market carry an appreciable risk of adverse impact upon the patient [3]. In order to analyze the interaction between SMA stents and the tunica interna with finite element methods, the hysteretic behavior of the SMA must be considered [68]. Doing so helps to reduce the likelihood and the severity of complications.

The industry has taken a great deal of this into account. By the middle of the 1990's, rates of ISR in BMS were around 25% [92]. While not perfect, advances in stenting have led to a reduction in ISR. For contemporary stenting with DES, that number is around 6% [7]. Still, the fact that one in twenty-four patients have to have a second emergency surgery as a result of poorly designed or poorly implanted stents drives the need for the research presented in this thesis.

This exemplifies the need for new materials and new processes of deployment for stents in order to reduce medical complications. In recent years, stents have been developed

using SMAs to address a few of these concerns. In fact, there have been several studies of SMA stents and their impact upon patient recovery as compared to traditional metal alloys [3] [93] [94]. In these studies, SMA stents are shown to be a viable medical solution in emergency stenting procedures.

SMA stents have been available on the market for a couple of decades, primarily comprised of the nickel-titanium alloy known as nitinol. Nitinol stents exhibit super-elastic and shape memory properties, contributing to superior characteristics for long-term stent implants [93]. These self-expanding stents have been proven to reduce the risk of restenosis compared to typical balloon angioplasty procedures and are a less invasive treatment option for the treatment of endovascular disease [95].

3.3 Design Approach

In this work, an SMA stent is designed for simulation in a human artery. While there are many factors to consider when designing such technology, it is important that the stent exhibit a series of crucial characteristics. These characteristics include good flexibility, ease of deliverability, the ability to withstand high radial forces, reasonable radio-opacity for x-ray imaging, and good biocompatibility [43]. These desired characteristics governed the approach to the stent design throughout the process.

The first major step in the design process was a study and literature review of current stent technologies, as evidenced by an extensive literature review section in this thesis. Key features were identified and considered in the process. While many stents are

manufactured with an open-cell design, which contributes to the flexibility of the stent, I chose to increase the rigidity of the stent by utilizing a closed-cell stent type. This reduces the risk of the stent collapsing after placement and causing ISR. This type of stent design is also easier to control with electrical during placement, as the expansion and collapse of each individual cell is similar to one another. This reduces the computing power required to simulate the behavior of the Flexinol stent and allows for a more accurate prediction of the behavior of the device.

The stent was originally designed in SolidWorks computer-aided design software for one-way simulation and ease of applying custom material properties to the stent. The proposed stent design utilizes a 150-micrometer diameter of wire to serve as the mesh tubing. This thickness was chosen because that is the diameter of the wire used in the wire contraction experiments. This mesh tube was cut to have an external surface that is more biocompatible with the inside of a human artery. In modern stent manufacturing, this is done by laser-cutting the cells into an extruded tube of metal. Figure 8 shows the stent designed in SolidWorks that serves as the primary CAD file for the simulations in this thesis.

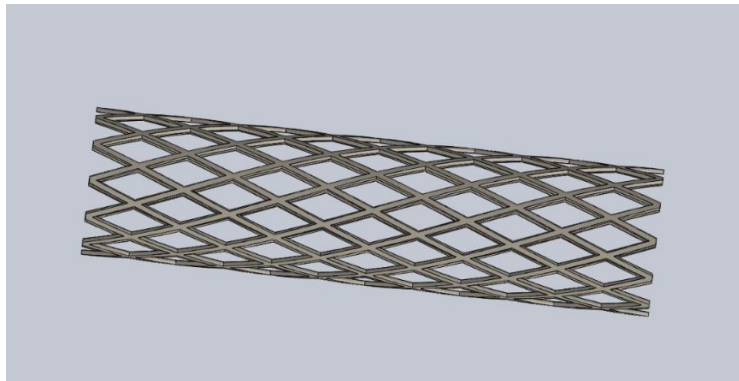


Figure 8. Stent design in SolidWorks.

This design incorporates the desire to model a stent for medium-sized arteries, while still being long enough to open stenosed arterial passages. The diameter of the stent model is 2.5 mm and the length is 10 mm. A shorter stent design was developed as a 5 mm length. One should note that these designs are typical of coronary stents and appreciate the miniscule size of these critical technologies.

The design shown in Figure 8 has closed cells to ensure that the stent does not collapse under the pressure of the surrounding arterial wall. It is important to simulate such interaction to verify the validity of using this device in medical applications.

3.4 Results and Discussion

In order to verify the viability of this stent design, finite element analysis (FEA) simulations were conducted to determine the stress and strain within the struts. Optimization with FEA has proven to be an efficient method of advancing and improving stent designs to exhibit desirable characteristics [65] [96] [97] [98] [99] [100]. Because of this, FEA serves as an important tool for determining the response of the stent in question and classifying its characteristics as an improvement upon current technologies. In FEA, complex domains are represented in discrete space via the use of elements which define the computational domain in such a way that a set of basis functions can be used to find the approximate solution of the original problem [5]. This is done through a process known as “meshing,” where the model is divided into a set of discrete elements prior to the

program solving the simulation for an answer at each element. SolidWorks FEA uses a built-in tool that allows users to validate their results by comparing them to analytical solutions of similar cases in the National Agency for Finite Element Methods and Standards database.

For this simulation, one end of the stent was fixed while the rest of the stent was allowed to react freely to external forces. A pressure equivalent to the average human blood pressure of 100 mmHg was placed upon the outside surface of stent to simulate interaction with the surrounding artery. In order to obtain meaningful results from the simulation, a fine tetrahedral solid mesh was used in the FEA, which is shown in the insert within Figure 9. This increased the number of nodes and elements and increased the computing power required to obtain results. Figure 9 demonstrates the setup of this FEA simulation. In this figure, the green arrows represent a fixed boundary condition and the red arrows signify the application of pressure on the external surface of the stent.

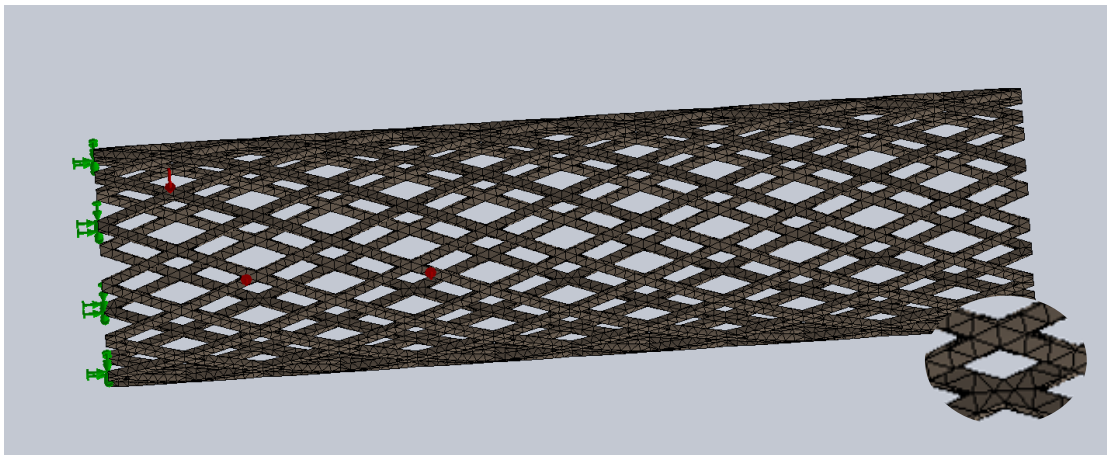


Figure 9. Boundary conditions and meshing in SolidWorks.

From here, the simulation was run to determine the stress in the struts and the connections, as well as predict the displacement of the stent when subjected to normal loading conditions. The results of this simulation are shown in Figure 10.

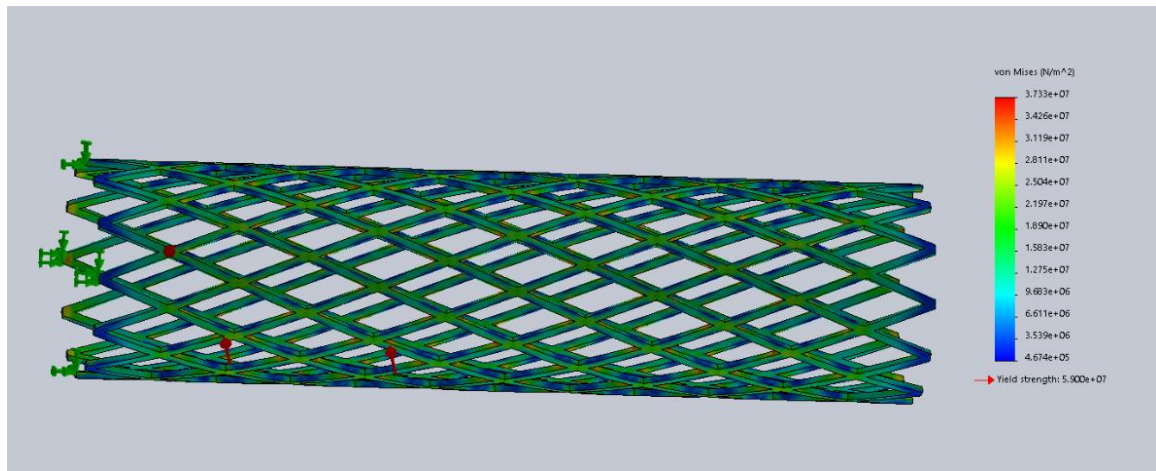


Figure 10. Von Mises stress in the stent when subjected to normal loading conditions.

As shown, the Von Mises stresses is highest at the strut connections. This stress is well below the yield strength of the material, which confirms that the proposed stent design is able to withstand the forces of the surrounding arterial wall. The stent experiences a maximum stress of about 37 MPa, which is lower than typical values for nitinol stents of various designs [3]. In fact, the simulations of the stent under maximum pressure had a factor of safety of approximately 1.6, which suggests that the stent, even with its small nature, is a robust solution to coronary artery blockages and stenosis.

When considering the stent, it is also important to investigate the displacement of the strut links when subjected to forces from the arterial wall. Large displacement indicates the likelihood of long-term deformation that could cause complications. As a result, it is crucial to run FEA to determine the stent behavior in this realm. Such simulations were conducted as part of this work. Results are shown in Figure 11.

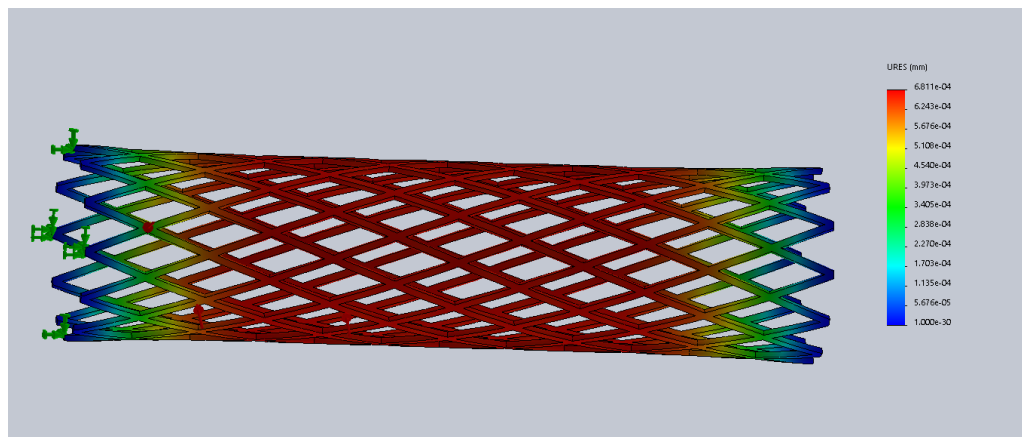


Figure 11. Displacement of the stent under normal loading conditions.

It can be seen that the maximum displacement of the stent under normal loading conditions is approximately 1 micrometer, which confirms that this stent design is a good choice for ensuring that stenosed arteries remain open. The stent itself is unlikely to experience any significant collapse after placement. This is extremely important, as it drastically reduces the risk of ISR.

3.5 Closure and Future work

The proposed stent design experiences low magnitudes of stress and strain, as verified by SolidWorks FEA simulations. Because of these characteristics, the proposed stent design is a durable choice to withstand long periods of time in the human body. This stent should not undergo as much fatigue as typical coronary artery stents, which translates to a longer life cycle. As a result of this longer life cycle, the proposed stent design will be able to stay in the body longer than the industry average of 10 years, thus reducing the likelihood of complications following a surgery to insert a new stent to reopen the affected artery.

The stent design analyzed in this chapter is also less prone to collapse compared to typical stents on the market today, as evidenced by the stress and strain simulations conducted in SolidWorks. The reduced likelihood of collapse ensures that a lower rate of ISR is likely with this design. As restenosis events are the most common complications associated with the placement of coronary artery stents, this Flexinol stent design will solve for the plurality of stent complications with proper implementation.

It is recommended that future work include FEA simulations with a variety of stent sizes and stent-artery boundary conditions. This work focuses upon the case of a stent placed in a medium-sized artery under normal operating conditions. In order to verify that this stent design is viable for larger arteries, additional simulations ought to be conducted with a larger stent file. Simulations including a variety of arterial boundary conditions could also be used to further validate this stent technology. Placing the stent under increased stress in order to mimic the conditions of extreme stenosis would be

beneficial toward that end. In either case, these additional simulations will require a great deal of computing power to yield meaningful results, as in the case of this chapter.

In conclusion, the design of Flexinol stents is not only possible, but actually superior to industry standard stent designs. By using a closed-cell design, the proposed stent has more rigidity, which decreases the likelihood of the medical condition of ISR. This stent design is therefore a beneficial BMS platform. Further simulations and study of this design will show the benefits of using Flexinol as a medium for this life-saving technology.

Chapter 4

Blood Flow through Flexinol Stent

4.1 Introduction

In order for the proposed stents to be validated as a solution for constricted arteries, it is necessary to simulate the flow of blood through such arteries before and after the placement of the stents. This chapter of the thesis is dedicated to research involving such simulation with the commercial computational fluid dynamics (CFD) software packages included in ANSYS Fluent.

This chapter presents the characteristics of each instance of blood flow through medium-sized arteries. This starts with a study of current literature on the structure of said arteries, as well as the flow of blood within. With this knowledge, the mathematical formulation of the blood flow is developed and presented. Flow characteristics are then used to perform CFD analysis of blood flowing through a stented artery in order to compare the simulated results with those of a healthy and unstented artery configuration.

It is important to understand the flow characteristics of normal blood flow, as well as the flow of blood through a stenosed artery. Comparing these with the simulation of an artery that has been stented with the proposed Flexinol stent, it is possible to verify the effectiveness of the stent and to investigate the impact the stent structure has on the stream of blood flowing through the arteries. To ensure a proper understanding of the aforementioned flow, the literature review in this chapter includes an examination of the arterial structure as well as the flow of blood through said arteries.

The simulation results will prove invaluable to the understanding of the flow of blood through stented arteries. Knowledge of particular flow patterns through stented arteries can aid in the design process to avoid critical medical conditions, including arterial ruptures. As a result, this chapter provides valuable insights into the medical viability of the proposed Flexinol-based BMS in clinical applications.

4.2 Literature Review

The first consideration in the complex nature of blood flow is that of the arteries themselves. Blood vessels exhibit highly nonlinear elastic behaviors owing to their complex material properties [101]. The behavior of individual blood vessels is dependent upon their structure and the materials that comprise each of their layers.

Large arteries are comprised of three major layers: the tunica externa, the tunica media, and the tunica interna. The tunica externa is primarily composed of loose connective tissue and is very flexible. The tunica media is comprised of smooth muscle fibers with various elasticities. The tunica interna is the layer of arterial tissue that directly contacts the flow of blood and is comprised of elastin fibers and simple squamous epithelium [102]. It is this layer that dictates the boundary conditions associated with the governing equations for the flow of blood through human arteries.

Figure 12 shows blood vessels both before and after a stenting operation. Part (A) displays a diseased coronary artery with lumen narrowed by presence of atherosclerotic plaque, part (B) shows that stent implementation causes severe injury to the vessel wall,

including endothelial denudation, resulting in platelet adhesion/activation with recruitment and activation of neutrophils, monocytes, and macrophages, part (C) demonstrates the release of cytokines and growth factors triggers smooth muscle cells to proliferate and migrate towards the lumen, and part (D) shows that the mature neointima is formed, comprising smooth muscle cells and extracellular matrix, covered by a restored endothelium [7].

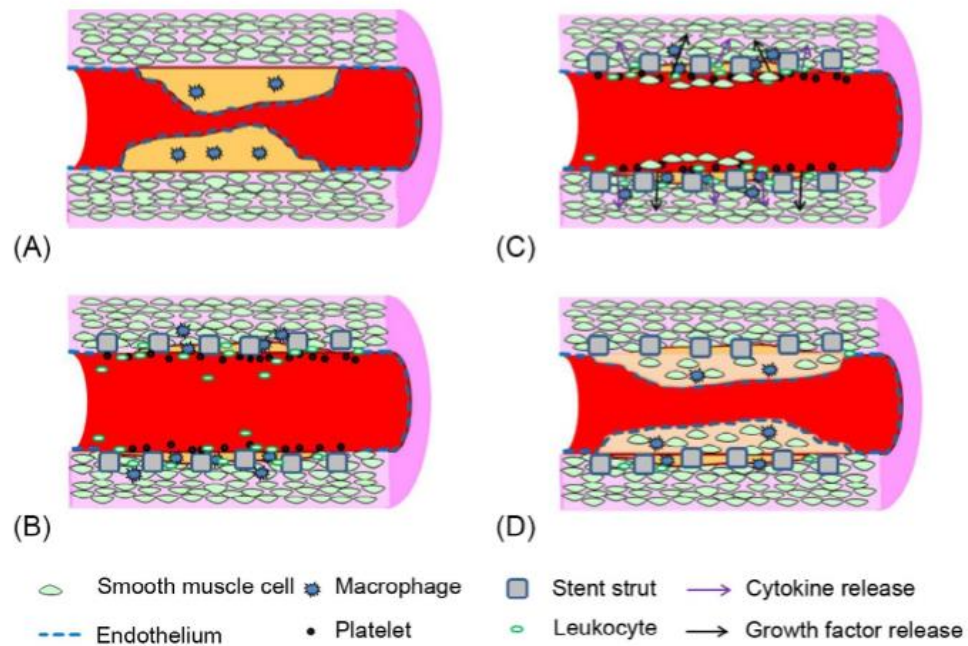


Figure 12. Schematic overview of in-stent restenosis. Figure shows key responses to stent implantation within a diseased coronary artery [103].

Because of the substantial amount of elastic tissue in larger blood arteries, the vessels expand and contract with the flow of blood. This elastic recoil produces a smoother

and more uniform flow of blood through the circulatory system, rather than pulsatile blood flow as it enters smaller arteries [102]. Therefore, stents placed in medium-sized arteries will not be subjected to flow patterns of an excessively pulsatile nature.

Smaller arteries are more rigid than their larger counterparts. As a result, they do not experience the same degree of expansion and contraction. However, while the flow of blood remains relatively constant through these portions of the cardiovascular network, the pressure within these arteries fluctuates in a pulsatile manner [102]. As the most common stenting procedure is performed on the arteries that lead to the legs, this thesis will examine the physiognomies of stent interaction within medium-sized arteries [48]. Concentrating the focus of this research upon these scenarios allows for the generation of knowledge that is most applicable to real-world scenarios. Such knowledge can be used as the basis for adapting the proposed stent design and placement procedure for use in a variety of biological applications.

Arterioles lack the muscle layer of the tunica media and capillaries are comprised only of a thin layer of squamous epithelium, also known as an endothelium [102]. This allows for cells to permeate the endothelium and oxygenate the local tissue. Blood vessels of this size are far too small for stenting procedures, and thus, will not be considered in this thesis.

There are a few other considerations for the development of the mathematical formulation of blood flow in human vessels. Arterial junctions provide a unique set of challenges, owing to the complex flow within [4]. In particular, arterial junctions often cause a great deal of swirling or other abnormal flow characteristics that can be difficult to

model. Additionally, stents placed near arterial junctions can disrupt the normal flow through the subsequent branches by diverting an imbalance of blood flow through one or more branches. In partially blocked coronary arteries, atherosclerosis causes abnormal blood flow patterns [6]. This imbalance of flow can lead to a variety of health issues, so it is important that the proposed stent design not cause a substantial disruption to the normal flow of blood through the affected arteries, especially in the vicinity of a significant arterial junction.

Arterial junctions, as well as arterial blockages, can also experience high concentrations of shear stress as a result of recirculation. Unlike veins, typical arteries do not have internal valves to stop the backflow of blood through the system [104]. The pressure of the blood being pumped from the healthy heart is enough to keep the flow moving in the correct direction. However, arterial junctions and constricted arteries can cause blood to swirl within the blood vessel. High vorticity of blood flow can shear layers at constricted portions of the artery, leading to uneven shear stresses within the blood vessel, which causes wear and subsequent rupture of the arterial wall [4]. Thus, laminar flow is desired.

As fluid flow is characterized by variations in pressure within the fluid, stenosis has a tremendous impact on the flow of blood through human arteries. As expected, unsteady Newtonian flow through a stenosed artery attains a peak pressure at the smallest cross-sectional area [105]. It has been observed that the pressure-drop increases with a reduction in the available cross-sectional area of an arterial passage [106]. Thus, the pressure of the blood decreases as the flow passes the blockage but increases in the artery near the constricted section. This variation in pressure throughout the artery impacts the flow of

blood as it passes through affected regions. The characteristics of this flow can have impacts on the health of the patient, including the likelihood of stroke, arterial ruptures, and several other medical conditions [107]. It is therefore crucial for the blood flow through the proposed stent to be similar to the flow of blood through a healthy artery.

Because the health of the involved patients is of paramount importance, predicting the patterns of blood flow through the implanted stent is crucial to the development of such stents [108]. The properties of the blood flowing through human arteries are extremely important for understanding the impact of the proposed stents. Even in stenosed arteries, the flow of blood tends to be laminar, with typical Reynolds numbers below 540 [6]. While blood is a non-Newtonian fluid, the behavior of its flow through arteries can be effectively modelled as Newtonian for simplicity [4]. This allows for a straightforward analysis of the flow patterns after the stent is placed.

Two-way fluid structure interaction between blood and the artery presents a basis for predicting the flow of blood with an assumption of non-Newtonian behavior. Utilizing pulsatile flow simulations, it is seen that recirculation effects increase as the arterial wall expands and contracts [109]. It makes sense that recirculation effects within smaller, more rigid, arteries are subjected to less recirculation effects than their elastic counterparts. For purposes of the simulations within this chapter, it is assumed that smooth, laminar flow enters the stented portion of the artery. This assumes that the arteries in question are negligibly elastic, and that they are far enough downstream of large elastic arteries to experience flow that is negligibly pulsatile. With these considerations, it is possible to construct straightforward mathematical formulations for the flow of blood through the

affected arteries and apply such formulations toward use in CFD simulations as a method of inspecting the stents' impact on the blood flow.

The flow of blood through arteries can follow complex patterns that have been studied through the use of a variety of mathematical models [110] [111] [112] [113]. Blood flow can change dramatically in arteries that have been subjected to plaque build-up or constriction, sometimes leading to unsteady flow [114] [115] [116] [117] [118]. The flow of blood also exhibits different characteristics in arteries that have been stented.

A recent thesis by a graduate student in the Department of Mathematics at the University of Groningen named de Bruin compiled a great deal of research on the blood flow through elastic vessels [119]. This research is a wonderful basis for the simulation of blood flow through human arteries.

To engage in the computational simulations necessary for this research, there are several considerations that must be noted. Finite element methods are powerful tools for approximating the solution of partial differential equations in which the boundary conditions are tremendously complex [86]. Many traditional mathematical approaches fail to achieve reasonable solutions to these types of problems. Due to the tremendous amount of computation power necessary to simulate three-dimensional FSI, utilizing image-based CFD or related discretized particle models is a difficult endeavor without reasonable simplification [1].

The simulations of blood flow in this chapter are three-fold. The first set of simulations involves a healthy, open artery in order to study normal blood flow conditions in the human body. The second set of simulations involves an artery that has been

stenosed or collapsed, which will reveal how blood travels through arteries that are constricted and in need of coronary stent procedures. Finally, the last set of simulations includes an artery that has been stented with the proposed stent design in order to validate its use as a viable technology for renormalizing the blood flow in affected regions of the cardiovascular system.

4.3 Mathematical Simulation of Blood Flow

For purposes of this study, I examine the case where the stent has been implanted in the artery and compare it to the normal flow of blood through a healthy artery. This approach assesses the implications of the stent while in use. By opening the artery, normal blood flow is restored. In cases such as this, blood flow through small or medium-sized arteries is typically laminar and three-dimensional flow, in which blood is considered to be incompressible [120]. Therefore, I can use the Navier-Stokes equations to govern the laminar flow of blood, which is a non-Newtonian, incompressible fluid. Utilizing continuity, I assume the following:

$$\frac{\partial u_i}{\partial x_i} = 0 \quad (28)$$

$$\rho_f \frac{\partial u_i}{\partial t} + \rho_f u_j \frac{\partial u_i}{\partial x_j} = -\frac{\partial}{\partial x_i} p + \frac{\partial}{\partial x_j} \left(\mu \frac{\partial u_i}{\partial x_j} \right) + F_i^{ext} \quad (29)$$

Where ρ_f is the density of the fluid, u_i is the velocity component of the fluid, F_i^{ext} is the external force, p is the pressure of the fluid, and μ is the fluid viscosity based on the Carreau model. [6]

$$\mu = \mu_\infty + (\mu_0 - \mu_\infty) \left\{ 1 + \left[\lambda \left(\sqrt{2 \sum_{i,j} S_{ij}^2} \right)^a \right]^{\frac{(n-1)}{a}} \right\} \quad (30)$$

Where μ_∞ is the infinite shear velocity, μ_0 is the zero shear velocity, a is the shape parameter, n is the index, λ is the time constant, and the function S_{ij}^2 is described below.

$$S_{ij}^2 = \frac{\left(\frac{\partial u_i}{\partial x_j} + \frac{\partial u_j}{\partial x_i} \right)^2}{4} \quad (31)$$

Using the conservation of momentum equations in normal blood flow, as in de Bruin's research, the following set of equations must hold true. These equations govern the behavior of blood as it flows through the arteries in the x, y, and z directions within the cartesian coordinate system. As shown, the flow is dependent upon the forcing function for each direction.

$$\frac{\partial u}{\partial t} + u \frac{\partial u}{\partial x} + v \frac{\partial u}{\partial y} + w \frac{\partial u}{\partial z} + \frac{\partial p}{\partial x} - \Upsilon \left(\frac{\partial^2 u}{\partial x^2} + \frac{\partial^2 u}{\partial y^2} + \frac{\partial^2 u}{\partial z^2} \right) = F_x \quad (32)$$

$$\frac{\partial v}{\partial t} + u \frac{\partial v}{\partial x} + v \frac{\partial v}{\partial y} + w \frac{\partial v}{\partial z} + \frac{\partial p}{\partial y} - \Upsilon \left(\frac{\partial^2 v}{\partial x^2} + \frac{\partial^2 v}{\partial y^2} + \frac{\partial^2 v}{\partial z^2} \right) = F_y \quad (33)$$

$$\frac{\partial w}{\partial t} + u \frac{\partial w}{\partial x} + v \frac{\partial w}{\partial y} + w \frac{\partial w}{\partial z} + \frac{\partial p}{\partial z} - \Upsilon \left(\frac{\partial^2 w}{\partial x^2} + \frac{\partial^2 w}{\partial y^2} + \frac{\partial^2 w}{\partial z^2} \right) = F_z \quad (34)$$

Where t represents time, p represents blood pressure, Υ is the kinematic viscosity. Much of the research does not include appreciable applied forces, such as gravity, so it can be approximated as zero. I set the forcing functions to be negligible, as external factors do not have a great impact on the flow of blood through human arteries.

Setting boundary conditions for the fluid flow simulations, the arterial walls included a no-slip condition. The condition at the outlet was set so that the fluid could be modeled as unidirectional, as per contemporary literature [119]. The mathematical formulation of such is presented in equation 35. For the sake of simplicity, ϑ is defined in equation 36. j represents the directional components of the outward pointing normal vectors at the outlet.

$$\frac{\partial \vartheta}{\partial j} = 0 \quad (35)$$

$$\vartheta = (u, v, w)^T \quad (36)$$

It is known that the flow velocity of blood is different at each point within the circulatory system. Smaller arteries typically have higher flow velocities as a result of the smaller cross-sectional area. In small and medium sized arteries, where the arterial wall can be assumed to be rigid, the flow velocity is relatively constant throughout the flood cycle. In these sections of the circulatory system, the velocity profile through a segment of the artery is independent of the upstream pulsatile motion of the flow. As a result, it is reasonable to model the flow of blood through such arteries as constant flow.

The density of blood is approximately 1055 kg/m^3 at normal body temperature [6]. This is the value that I chose to use for my simulations. The CFD software used in this thesis utilizes this set of equations to solve for the fluid flow at any point in the artery. There are other parameters that need to be considered in order to setup a complete flow simulation. Among these are the Reynolds number of the flow, which I took to be equal to 1200, which is the maximum Reynolds number of steady-state blood flow through human arteries. It is also important to determine the typical fluid velocity of the flow of blood through an artery. This is dependent upon the size and location of the blood vessel within the human body. For the purposes of this thesis research, the arterial case that is studied can be assumed to have a maximum flow velocity of approximately 0.1 m/s through the interior [121]. CFD simulations shown within this thesis are based upon these experimentally derived values for the properties of blood within a human artery.

4.4 CFD Model Setup and Validation

CFD simulations were conducted in order to analyze the flow effects of the proposed stent design. For the purposes of this analysis, three separate scenarios were modeled in AutoDesk Inventor CAD software. These CAD models were then discretized with a set of mesh parameters in ANSYS commensurate with studies of blood flow through human arteries with a finer mesh surrounding areas of particular interest to this study [122]. The CFD simulations were validated by using the same meshing parameters as an existing study that uses ANSYS Fluent to examine blood flow through an arterial section [123]. The walls of such arteries are semi-rigid and were assigned properties to model them like so. Each CAD model was drafted to the same dimensions, including length, diameter, and wall thickness. This ensures that the results gleaned from CFD simulations are truly comparable analyses that provide valuable information regarding the flow characteristics in medium-sized sections of human arteries.

Flow simulations were conducted in ANSYS Fluent. Each case was setup in a similar manner. The most important of these is the stented case and its comparison to the others. In this instance, a fine mesh was utilized at the location of the implanted stent in order to provide better results. Blood flow through the CAD models was set for standard conditions, including a typical human body temperature of 310 K and a viscosity of 0.002. The inlet flow condition was modeled as steady-state flow with a constant centerline velocity of 0.15 m/s in order to simulate an appropriate scenario in accordance with typical human biology. A roughness factor of 0.01 was selected for the inside of the arterial wall to be an approximate average roughness coefficient across typical biological material. The roughness factor of the Flexinol was based upon the values provided by the manufacturer

of the wires. From here, a set of 150 simulations was run for each case, with the composite results collected for analysis. There is a one particular characteristic of the blood flow that is of utmost importance for determining the impact of the use of the proposed stent design in clinical applications. Specifically, the pressure distribution is a key indicator of potential thrombosis.

The setup of the CFD models was done with similar mesh parameters to the aforementioned reference case. For purposes of model verification, the tetrahedral mesh parameters were adjusted to replicate the conditions present in the blood flow simulations. Figure 13(a) shows the reference artery with its mesh. Figure 13 (b) compares both versions of the displacement results of an ANSYS Fluent 16.2 simulation of this case using a section of the model, with the mesh parameters and boundary conditions present in this study.

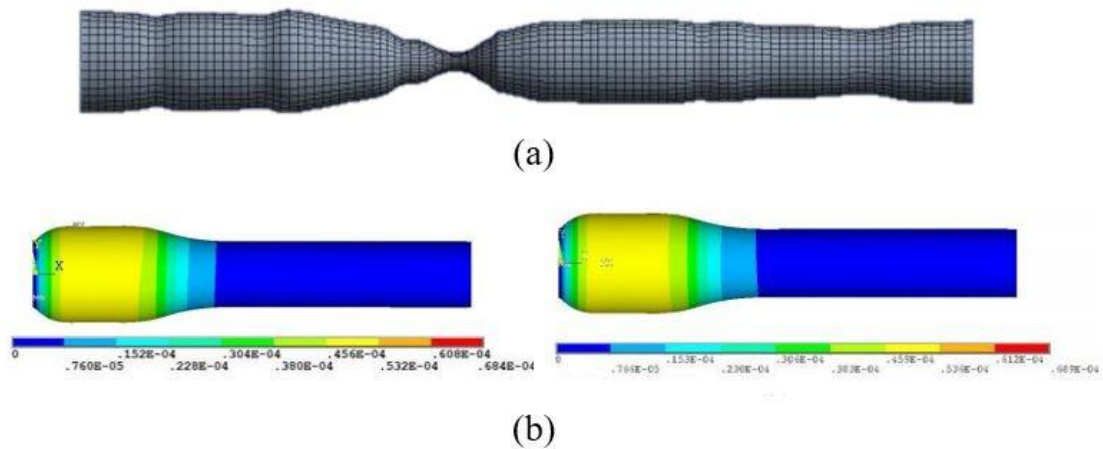


Figure 13. CFD model verification.

The CFD models were further validated an examination of iterative convergence. The simulations were set to run 150 times in order to examine the convergence of the simulation results. The convergence plots indicate that the solution converged within 80 iterations, which signifies that the CFD is solvable to a reasonable solution. The simulations were checked for consistency by confirming the confirmation of mass.

As previously discussed, three cases are of interest for this study. The CAD models of the each of these cases are shown in Figure 14 for reference. The CAD models were designed in AutoDesk Inventor and exported as STP files for use as the geometry models for ANSYS Fluent simulations of blood flow.

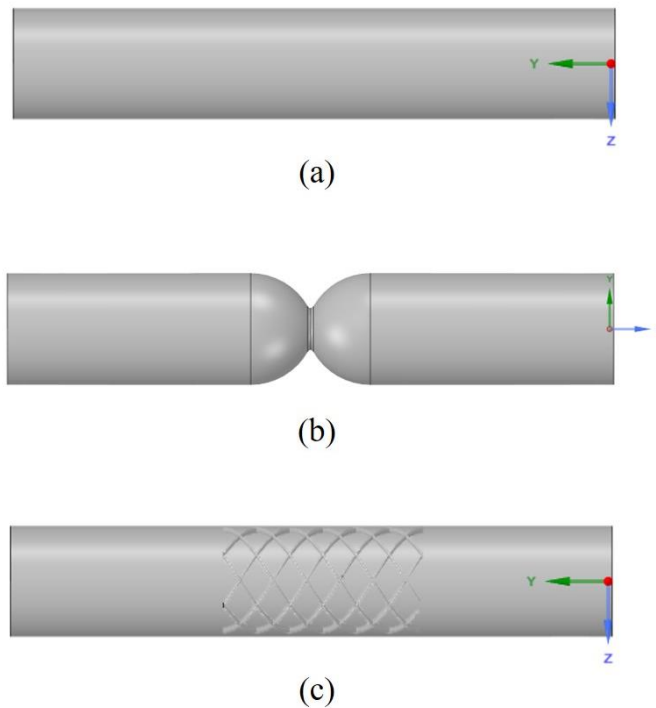


Figure 14. Computer-aided design models of each artery case. (a) Healthy artery, (b) stenosed artery, (c) stented artery.

4.5 Results and Discussion

The first case represents a healthy artery, the second represents an artery with a stenosis of approximately 60%, and the final scenario represents an artery with an implanted Flexinol stent. Each of these arterial section models were designed to simulate the real-world situation with a medium-sized artery in the human body. The first set of results presented below represents the pressure on the arterial wall. Due to bugs with the ANSYS software, the resulting simulation images were unable to be set to similar scales. Figures 15-17 below demonstrate the pressure distributions across the arterial wall in all three cases that warrant examination.

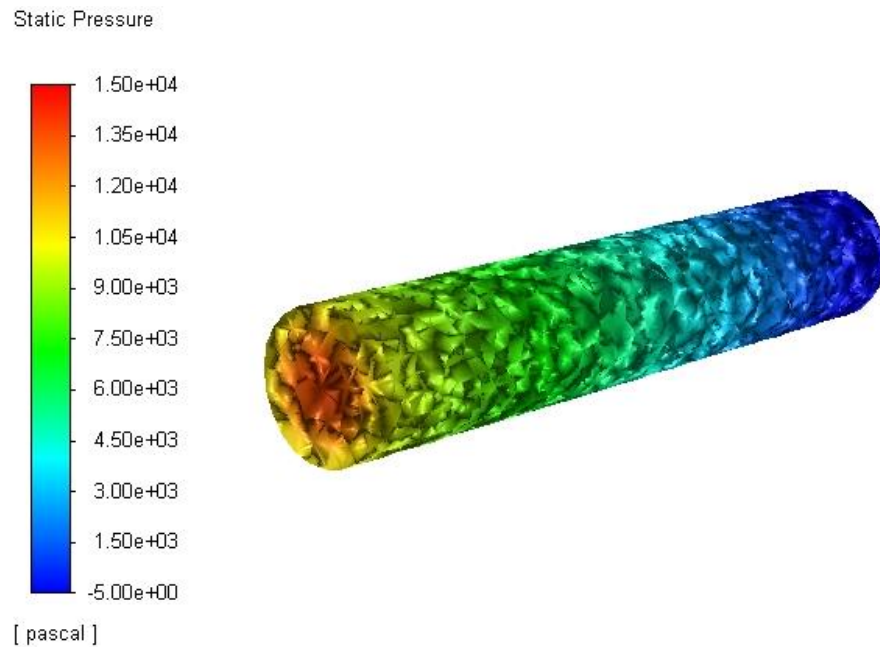


Figure 15. Static pressure distribution for the healthy artery case.

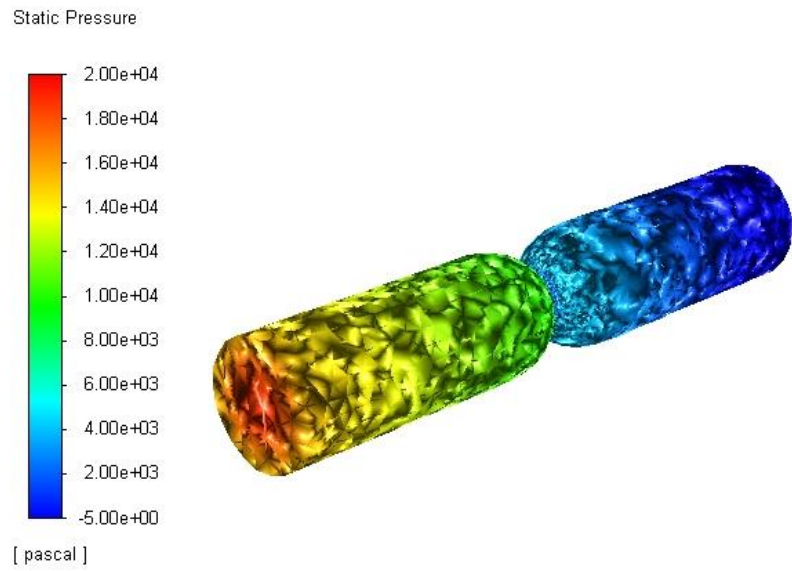


Figure 16. Static pressure distribution for stenosed artery case.

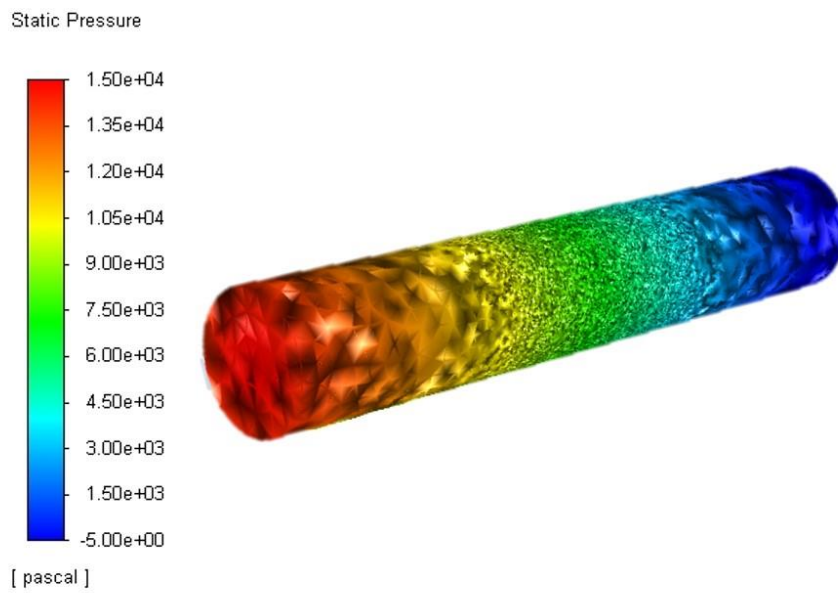


Figure 17. Static pressure distribution for stented artery case.

As shown in Figure 15, the magnitude of the pressure decreases as the blood flows through the artery, which is to be expected. Fluids flow from areas of high pressure to low pressure. In this case, the maximum static pressure within the arterial wall is less than 1.5 kPa, which is in the normal range for human arteries.

This increases in the stenosed case, which is displayed in Figure 16. As shown, the pressure within the artery builds ahead of the stenosis, creating a large pressure differential between the upstream and downstream sections. This large static pressure difference contributes to abnormal flows and the generation of aneurysms. This is also an early sign of potential thrombosis within the artery itself. The maximum pressure in this case is approximately 2 kPa, which is a 33% increase from the healthy case. A stenosis of this type can cause deadly consequences with the increased pressure, so it is important that the pressure be reduced by implanting an arterial stent.

The stented artery case is shown in Figure 17. As displayed, the pressure distribution through the artery is scaled similarly to the healthy case, and the simulation shows that the maximum pressure is similar in the two cases. This is a result of the revascularization of the stenosed artery, which restores the artery to a state that is comparable to a healthy blood vessel. The high-pressure region is larger in this case than the healthy case, which is to be expected, due to the stent creating a minor obstruction within the artery. However, the pressure drop across the artery section is much smaller than the unhealthy case. In fact, Figure 17 displays a smooth pressure drop across the stent, as opposed to the stenosed case, where there is an abrupt pressure change at the site of the stenosis. As shown, the stent design considered in this study is able to restore the flow of blood to healthy pressure distributions.

4.6 Closure and Future Work

Through the use of ANSYS CFD simulations, it is shown that the proposed stent design is a great candidate for revascularization procedures to restore the flow of blood to affected arteries. The simulation results show that the stenosed artery case increases the maximum pressure by over 30%, which is very dangerous if sustained for a long period of time. The simulation results of the stented artery case demonstrate the stent's ability to reestablish healthy pressure distribution within the artery.

In future work, this study of the proposed stent design could be applied to broader studies of the effects of the strut shapes on the flow of blood through the artery. The findings from this thesis may be compared to additional studies on contemporary stent designs, such as the studies by Lally, et al. and Li et al., among others [41] [77]. Such a study is out of the scope of this research but will serve to further the contemporary knowledge of how different stent designs impact the distribution of blood pressure through the affected region of a stented artery. Further research may involve the use of open-celled stent designs for added flexibility in the stent structure, which would allow for placement of Flexinol stents in biological locations that undergo an appreciable amount of movement.

Chapter 5

Concluding Remarks and Future Work

5.1 Key Results

The valuable research presented within this thesis demonstrates the viability of Flexinol as an SMA stenting platform. The presented research includes an experimentally verified mathematical model governing the contraction behavior of Flexinol that serves as the basis for further advances in the use of the material in engineering applications. By demonstrating the predictability of the material, it is shown to be controllable for actuation.

This principle was applied through the design of an SMA stent with the properties of Flexinol. Implementing a closed cell stent design for the proposed BMS platform, it was shown that the design exhibits low stresses when subjected to typical loading conditions. This signifies that the stent developed in this study is likely to retain its deployed configuration without significant deformation, in turn reducing occurrences of the critical condition known as restenosis.

Further, the ANSYS CFD simulations demonstrated the effectiveness of the proposed stent in restoring blood flow in diseased arteries. The pressure patterns present in the stented artery models indicate that the proposed stent is a viable option for use in PCI operations.

In sum, this research demonstrates that the SMA Flexinol can be utilized as a controllable method of actuation in small robotic applications. This work shows the viability of its use as a BMS stenting platform that can be controlled during deployment to

reduce the likelihood of complications resulting from improperly placed stents. These complications are further reduced by the demonstrated durability of the stent design developed within this work.

5.2 Application of Machine Learning

It is recommended that the proposed stent design be utilized in conjunction with advanced machine learning techniques to improve success rates for the applicable procedures. In particular, it will prove beneficial to incorporate classification algorithms in the selection of the optimum stent dimensions. As previously stated, incorrect stent sizing can cause a multitude of serious medical complications, including the potentially deadly conditions of restenosis and thrombosis [59] [60]. Because of the likelihood of human error in the selection of correct stent size for a given arterial application, it will prove advantageous to automate the process.

Machine learning is a subset of soft artificial intelligence that involves computers gathering information to perform a particular task. In such applications, the computer produces better results with a greater quantity or quality of input data. Machine learning can be used in a variety of ways to provide valuable advancement of the commercial use of the stents developed in this thesis. Namely, machine learning can be used as a predictive mechanism or as a classification algorithm. In fact, some work has been done to predict turbulent fluid flow that could be applied to assist doctors that are examining radiological imaging of stenosed or diseased arteries, among these are a doctoral dissertation on such [124]. There has also been valuable research presented in a conference paper on the use of

magnetic imaging to predict turbulent flows. These two will prove incredibly useful to researchers that wish to understand the effects of constricted arteries on the flow of blood through the body [125]. This information can be used to predict or simulate the flow and identify regions of high shear stress that may require additional stenting solutions.

The second type of machine learning that ought to be implemented in future Flexinol stent research is that of classification. In this type of machine learning, a computer is provided with a set of data or images with defined characteristics and tasked with classifying new images or data into sets that correspond with practical categories. For the purposes of this research, it is recommended that images of stenosed arteries be uploaded into the computer with a classification learning algorithm along with corresponding dimensional data. Of course, the computer also requires the desired solution to each of these problems before it can learn what to do with the information. This will take the form of a set of stent dimensions for the stents that are successfully placed in the stenosed arteries. With this information, the computer will learn to classify new patient images into categories that correspond with different sizes of Flexinol stents, which can prove a valuable tool to reduce human error in the selection of stenting platforms for patients undergoing critical surgeries to reopen stenosed arteries.

5.3 Closure

This research advances crucial knowledge of SMA behavior and its applications in modern engineering technologies. In particular, this thesis develops models for controlling the actuation of Flexinol SMA wires and applies such findings to life-saving biomedical

applications. The valuable research presented within this thesis demonstrates the viability of Flexinol as an SMA stenting platform. This advancement of knowledge in the area of SMAs serves as a basis for additional research and applications in the biomedical field. The utilization of electrically-controlled Flexinol wire as a BMS stenting platform is an innovative solution to address complications surrounding the use of typical stenting technologies.

Chapter 2 involved the development and experimental verification of constitutive equations for the electrothermal contraction behavior of the SMA Flexinol. Such research advances our understanding of SMA behavior and allows for the further development of control mechanisms for utilizing SMA wires as sources of mechanical actuation in mechanical engineering applications.

The third chapter of this work presented the practical application of the SMA Flexinol as a platform for BMS technologies. The research presented includes SolidWorks CAD modeling and FEA simulation of the stress loads when working conditions are applied, which reveals the response behavior of the proposed stent design. With the FEA verification that the Flexinol stent design will be able to sustain normal working conditions once implanted into the human body, one can see that the proposed low stress design has the potential to reduce the rate of stent failure in comparison to typical technologies available on the market.

Chapter 4 included a valuable study of the blood flow patterns and associated fluid-structure interaction through the implanted Flexinol stent. The ANSYS Fluent CFD solutions demonstrated the stent's impact on restoring the flow of blood through a stenosed

artery to that of a healthy artery. The simulations also showed minimal turbulence in the stented region, which corresponds to lower stresses in the arterial wall and a reduced likelihood of thrombosis as compared to typical stent designs.

The fifth chapter suggested areas of advancement for Flexinol stent technologies through the use of machine learning to select stent designs and summarized the key results from this research. Such research will build upon the crucial work presented in this thesis and will grow from the successful development of the Flexinol stent technology presented in this composition.

In its entirety, the work presented within this thesis demonstrates that the SMA Flexinol can be utilized as a controllable method of actuation, which has broad implications in the engineering disciplines. Applying such knowledge to the biomedical field in particular, this research shows the viability of using Flexinol as the platforming for BMS technology that can be controlled during deployment to reduce the likelihood of complications. The proposed Flexinol stent has the prospect of further reducing medical complications through its demonstrated characteristics. This can have massive implications for the biomedical industry and the treatment of the world's most lethal diseases.

References

- [1] T. A. Gaziano, A. Bitton, S. Anand, S. Abrahams-Gessel and A. Murphy, "Growing Epidemic of Coronary Heart Disease in Low- and Middle-Income Countries," *Current Problems in Cardiology*, vol. 35, no. 2, pp. 72-155, 2010.
- [2] S. Mendis, P. Puska and B. Norrving, "Global Atlas on Cardio-Vascular Disease Prevention and Control," World Health Organisation in collaboration with World Heart Federation and World Stroke Organisation, Geneva, Switzerland, 2011.
- [3] T. Roy and A. Chanda, "Computational Modelling and Analysis of Latest Commercially Available Coronary Stents During Deployment," *Procedia Computer Science*, vol. 5, pp. 2310-2319, 2014.
- [4] D. Sarkar, N. Upadhyay, S. Roy and S. C. Rana, "Immersed Boundary Simulation of Flow Through Arterial Junctions," *Sadhana*, vol. 42, pp. 533-541, 2017.
- [5] C. F. Carmen, A. Stelian, C. M. Catalina, I. Luminita and C. D. Aurora, "Finite Element Analysis For A Simplified Model Of A Blood Vessel With Lesion," *Annals of The Oradea University, Fascicle of Management and Technological Engineering*, vol. 9, no. 19, 2010.
- [6] M. Kaewbumrung, S. Orankitjaroen, P. Boonkrong, B. Nuntadilok and B. Wiwatanapataphee, "Numerical Solution of Dispersed Particle-Blood Flow in the Stenosed Coronary Arteries," *International Journal of Differential Equations*, vol. 2018, pp. 1-16, 2018.
- [7] C. McCormick, "Overview of Cardiovascular Stents," in *Functionalized Cardiovascular Stents*, Elsevier, 2018, pp. 3-26.
- [8] A. Kalyanasundaram and J. Blankenship, "Comparison of Coronary Artery Bypass Grafting (CABG) and Percutaneous Coronary Intervention (PCI)," *Drugs, Diseases, and Procedures*, 2014.
- [9] P. Serruys, P. de Jaegere, F. Kiemeneij, C. Macaya, W. Rutsch, G. Hendrickx, H. Emmanuelsson, J. Marco, V. Legrand and P. Materne, "A Comparison of Ballon-Expandable Stent Implementation with Balloon Angioplasty in Patients with Coronary Artery Disease," *New England Journal of Medicine*, vol. 331, no. 8, pp. 489-495, 1994.
- [10] U. Sigwart, "Stents: a mechanical solution for a biological problem?," *European Heart Journal*, vol. 18, pp. 1068-1072, 1997.
- [11] R. A. Byrne, P. W. Serruys, A. Baumbach, J. Escaned, J. Fajadet, S. James, M. Joner, S. Oktay, P. Juni, A. Kastrati, G. Sianos, G. Stefanni, W. Wijns and S. Windecker, "Report of a European Society of Cardiology-European Association of Percutaneous Cardiovascular Interventions Taskforce on the Evaluation of Coronary Stents in Europe: Executive Summary," *European Heart Journal*, vol. 36, no. 38, pp. 2608-2620, 2015.

- [12] Boston Scientific, "How Coronary Stents Work," Boston Scientific, [Online]. Available: www.bostonscientific.com/content/gwc/en-US/patients/about-your-device/coronary-stents/how-coronary-stents-work.html. [Accessed 24 August 2018].
- [13] B. K. Itagaki and S. S. Brar, "Controversies in the Use & Implementation of Drug-Eluting Stent Technology," *Indian Journal of Medical Research*, vol. 136, no. 6, pp. 926-941, 2012.
- [14] T. W. W. M. Duering, "A Comparison of Balloon- and Self-Expanding Stents," *Minimally Invasive Thermal Allied Technology*, vol. 11, no. 4, pp. 173-178, 2002.
- [15] D. Fischman, M. Leon and D. Baim, "A Randomized Comparison of Coronary Stent Placement and Balloon Angioplasty in the Treatment of Coronary Artery Disease," *New England Journal of Medicine*, vol. 331, pp. 496-501, 1994.
- [16] M. Leon and A. Bakhai, "Drug-eluting Stents and Glycoprotein Inhibitors: Combination Therapy for the Future," *American Heart Journal*, vol. 146, no. 4, pp. S13-7, 2003.
- [17] A. A. Bavry, D. J. Kumbhani, T. J. Helton and D. L. Bhatt, "Risk of Thrombosis with the Use of Sirolimus-Eluting Stents for Percutaneous Coronary Intervention," *American Journal of Cardiology*, vol. 95, pp. 1469-1472, 2005.
- [18] GlobalData MediPoint, "Coronary Stents – Global Analysis and Market Forecasts," GlobalData, 2014.
- [19] R. Kornowski, M. K. Hong, F. O. Tio, O. B. Bramwell, W. H and e. al, "In-Stent Restenosis: Contributions of Inflammatory Responses and Arterial Injury to Neointimal Hyperplasia," *Journal of the American College of Cardiology*, vol. 31, pp. 224-230, 1998.
- [20] B. Thierry, Y. Merhi, L. Bilodeau, C. Trepanier and M. Tabrizian, "Nitinol Versus Stainless Steel Stents: Acute Thrombogenicity Study in an ex vivo Porcine Model," *Biomaterials*, vol. 23, no. 14, pp. 2997-3--5, 2002.
- [21] L. H. Arroyo and R. T. Lee, "Mechanisms of Plaque Rupture: Mechanical and Biologic Interactions," *Cardiovascular Research*, vol. 41, pp. 369-375, 1999.
- [22] P. Douglas, J. Brennan and K. Anstrom, "Clinical Effectiveness of Coronary Stents in the Elderly: Results from 262,700 Medicare Patients in ACC-NDCR," *Journal of the American College of Cardiology*, vol. 53, pp. 1629-1641, 2009.
- [23] S. Pant, N. Bressloff and G. Limbert, "Geometry Parameterization and Multidisciplinary Constrained Optimization of Coronary Stents," *Biomechanics and Modelling in Mechanobiology*, vol. 11, no. 1-2, pp. 61-82, 2012.
- [24] E. Peterson, P. Cowper, E. DeLong, J. Zidar, R. Stack and D. Mark, "Acute and Long-Term Cost Implications of Coronary Stenting," *Journal of the American College of Cardiology*, vol. 33, pp. 1610-1618, 1999.
- [25] P. Grewe, T. Deneke, A. Machraoui, J. Barmeyer and K. Muller, "Acute and Chronic Tissue Response to Coronary Stent Implantation: Pathologic Findings in Human Specimens," *Journal of the American College of Cardiology*, vol. 35, pp. 157-163, 2000.

- [26] E. Edelman and C. Rogers, "Pathobiologic Responses to Stenting," *American Journal of Cardiology*, vol. 1998, pp. 4E-6E, 1998.
- [27] R. Hoffman, G. S. Mintz, R. Mehran, K. M. Kent, A. D. Pichard, L. F. Satler and M. B. Leon, "Tissue Proliferation within and Surrounding Palmaz-Schatz Stents is Dependent on the Aggressiveness of the Stent Implantation Technique," *American Journal of Cardiology*, vol. 83, pp. 1170-1174, 1999.
- [28] K. Arakawa, K. Isoda, Y. Sugiyabu, M. Fukuda, K. Nishizawa, T. Shibuya and H. Nakamura, "Intimal Proliferation After Stenting Reflected by Increased Stent-to-Vessel Cross-Sectional Area Ratio: Serial Intravascular Ultrasound Study," *Journal of Cardiology*, vol. 32, pp. 379-389, 1998.
- [29] R. Schwartz and D. Holmes, "Pigs, Dogs, Baboons, and Man: Lessons in Stenting from Animal Studies," *Journal of Interventional Cardiology*, vol. 7, pp. 355-368, 1994.
- [30] C. Rogers and E. Edelman, "Endovascular Stent Design Dictates Experimental Restenosis and Thrombosis," *Circulation*, vol. 91, pp. 2995-3001, 1995.
- [31] A. Kastrati, J. Dirschinger, P. Boekstegers, S. Elezi, H. Schühlen, J. Pache, G. Steinbeck, C. Schmitt, K. Ulm, F. Neumann and A. Schomig, "Influence of Stent Design on 1-Year Outcome After Coronary Stent Placement: a Randomized Comparison of Five Stent Types in 1,147 Unselected Patients," *Catheterization and Cardiovascular Interventions*, vol. 50, pp. 290-297, 2000.
- [32] A. C. Morton, D. Crossman and J. Gunn, "The Influence of Physical Stent Parameters upon Restenosis," *Pathologie Biologie*, vol. 52, no. 4, pp. 196-205, 2004.
- [33] M. Lucci, J. Oyedele and C. H. Goh, "An Integrated Design Teaching Approach to Student Understanding of Material Behavior in the Area of Shape Memory Alloys," in *American Society of Engineering Education Gulf Southwest Conference Proceedings*, Tyler, Texas, 2019.
- [34] G. Lange, A. Lachmann, A. Rahim, M. Ismail and C. Low, "Shape Memory Alloys as Linear Drives in Robot Hand Actuation," *Procedia Computer Science*, vol. 76, pp. 168-173, 2015.
- [35] J. T. Hogan, "Self-Expanding Stent with Enhanced Radial Expansion and Shape Memory". United States of America Patent US6569191, 27 May 2003.
- [36] J. D. Unsworth and T. C. Waram, "Shape Memory Tubular Stent". United States of America Patent 6635079, 21 October 2003.
- [37] F. Gori, D. Carnevale, A. Doro Altan, S. Nicosia and E. Pennestri, "Gori, F., Carnevale, D., DorA New Hysteretic Behavior in the Electrical Resistivity of Flexinol Shape Memory Alloys Versus Temperature," *International Journal of Thermophysics*, vol. 27, pp. 866-879, 2006.
- [38] B. Lynch, "Modeling of the Stress-Strain-Resistance Behaviour of Ni-Ti and Ni-Ti-Cu Shape Memory Alloys for use in Sensorless Actuator Position Control," Carlton University, 2013.

- [39] H. Song, E. Kubica and R. Gorbet, "Resistance Modelling of SMA Wire Actuators," in *Smart Materials, Structures & NDT in Aerospace Conference. NDT in Canada.*, 2011.
- [40] J. Bittle, "Bioresorbable Stents: The Next Revolution," *Circulation*, vol. 122, pp. 2236-2238, 2010.
- [41] J. Li, F. Zheng, X. Qiu, P. Wan, L. Tan and K. Yang, "Finite Element Analyses for Optimization Design of Biodegradable Magnesium Alloy Stent," *Materials Science and Engineering C*, vol. 42, pp. 705-714, 2014.
- [42] H. Hermawan, D. Dube and D. Mantovani, "Developments in metallic biodegradable stents," *Acta Biomaterialia*, vol. 6, pp. 1693-1697, 2010.
- [43] B. Tomberli, A. Mattesini, G. I. Baldereschi and C. Di Mario, "A Brief History of Coronary Artery Stents," *Revista Española de Cardiología*, vol. 71, no. 5, pp. 312-319, 2018.
- [44] D. Kereiakes, I. Meredith, S. Windecker, R. Lee Jobe, S. R. Mehta, I. J. Sarembock, R. L. Feldman, B. Stein, C. Dubois, T. Grady, S. Saito, T. Kimura, T. Christen, D. Allocco and K. D. Dawkins, "Efficacy and Safety of a Novel Bioabsorbable Polymer-Coated, Everolimus-Eluting Coronary Stent: the EVOLVE II Randomized Trial," *Circulation: Cardiovascular Interventions*, vol. 8, no. 4, pp. 1-8, 2015.
- [45] S. Windecker, P. Serruys and S. Wandel, "Biolimus-Eluting Stent with Biodegradable Polymer Versus Sirolimus-Eluting Stent with Durable Polymer for Coronary Revascularisation (LEADERS): a Randomised Non-Inferiority Trial," *Lancet*, vol. 372, pp. 1163-1173, 2008.
- [46] C. Di Mario, P. Serruys and S. Silber, "Long-Term Outcome After Zotarolimus-Eluting Stent Implantation in Patients with ST-Segment Elevation Acute Myocardial Infarction: Insights from the RESOLUTE All Comers Trial and the RESOLUTE Global Clinical Trial Program," *EuroIntervention*, vol. 12, pp. 1207-1214, 2016.
- [47] P. Karjalainen, W. Namas and J. Airaksinen, "Optimal Stent Design: Past, Present & Future," *Interventional Cardiology*, vol. 6, no. 1, pp. 29-44, 2014.
- [48] J. H. Lee, E. D. Kim, E. J. Jun, H. S. Yoo and J. W. Lee, "Analysis of Trends and Prospects Regarding Stents for Human Blood Vessels," *Biomaterials Research*, vol. 22, no. 8, pp. 1-10, 2018.
- [49] T. Wang, Z. Shi, D. Liu, C. Ma and Z. Zhang, "An Accurately Controlled Antagonistic Shape Memory Alloy Actuator with Self-Sensing," *Sensors*, vol. 12, pp. 7682-7700, 2012.
- [50] L. Lecce and A. Concilio, *Shape Memory Alloy Engineering for Aerospace, Structural, and Biomedical Applications*, Oxford: Elsevier, 2015.
- [51] N. Ma and G. L. H. Song, "Position control of shape memory alloy actuators with internal electrical resistance feedback using neural networks," *Smart Material Structures*, vol. 13, pp. 777-783, 2004.

- [52] M. Carballo, Z. J. Pu and K. H. Wu, "Variation of Electrical Resistance and the Elastic Modulus of Shape Memory Alloys under Different Loading and Temperature Conditions," *Journal of Intelligent Material System Structures*, vol. 6, pp. 557-565, 1995.
- [53] A. Hadi, A. Yousefi-Koma, M. M. Moghaddam, M. Elahinia and A. Ghazavi, "Developing a Novel SMA-Actuated Robotic Module," *Sensors and Actuators A: Physical*, vol. 162, pp. 72-81, 2010.
- [54] Y. Teh and R. Featherstone, "An Architecture for Fast and Accurate Control of Shape Memory Alloy Actuators," *International Journal of Robotics Research*, vol. 27, pp. 595-611, 2008.
- [55] A. Nespoli, S. Besseghini, S. Pittaccio, E. Villa and S. Viscuso, "The High Potential of Shape Memory Alloys in Developing Miniature Mechanical Devices: A Review on Shape Memory Alloy Mini-Actuators," *Sensors and Actuators A: Physical*, vol. 158, pp. 149-160, 2010.
- [56] P. Sittner, G. Dayananda, F. Brz-Fernandes, K. Mahesh and V. Novak, "Electric Resistance Variation of NiTi Shape Memory Alloy Wires in Thermomechanical Tests: Experiments and Simulation," *Materials Science and Engineering A*, vol. 481, pp. 127-133, 2008.
- [57] J. M. Jani, M. Leary, A. Subic and M. Gibson, "A Review of Shape Memory Alloy Research, Applications and Opportunities," *Materials & Design*, vol. 56, pp. 1078-1113, 2013.
- [58] Dynalloy Inc., *Technical Characteristics of Flexinol Actuator Wires*, 2009.
- [59] R. Hoffman, G. S. Mintz, G. R. Dussailant, J. J. Popma, A. D. Pichard, L. F. Satler, K. M. Kent, J. Griffin and M. B. Leon, "Patterns and Mechanisms of In-Stent Restenosis: A Serial Intravascular Ultrasound Study," *Circulation*, vol. 94, pp. 1247-1254, 1996.
- [60] A. Mitra and D. Agrawal, "In Stent Restenosis: Bane of the Stent Era," *Journal of Clinical Pathology*, vol. 59, pp. 232-239, 2006.
- [61] R. Virmani, G. Guagliumi, A. Farb, G. Musumeci, N. Grieco, T. Motta, L. Mihalcsik, M. Tespili, O. Valsecchi and F. D. Kolodgie, "Localized Hypersensitivity and Late Coronary Thrombosis Secondary to a Sirolimus-Eluting Stent: Should We Be Cautious?," *Circulation*, vol. 109, pp. 701-705, 2004.
- [62] R. Koster, D. Vieluf, M. Kiehn, M. Sommerauer, J. Kahler, S. Baldus, T. Mienertz and C. W. Hamm, "Nickel and Molybdenum Contact Allergies in Patients with Coronary In-Stent Restenosis," *The Lancet*, vol. 356, pp. 1895-1897, 2000.
- [63] R. Waksman, "Update on Bioabsorbable Stents: From Bench to Clinical," *Journal of Interventional Cardiology*, vol. 19, pp. 414-421, 2006.
- [64] B. Heublein, R. Rohde, V. Kaese, M. Niemeyer, W. Hartung and A. Haverich, "Biocorrosion of Magnesium Alloys: a New Principle in Cardiovascular Implant Technology?," *Heart*, vol. 89, pp. 651-656, 2003.
- [65] W. Wu, D. Gastaldi, K. Yang, L. Tan, L. Petrini and F. Migliavacca, "Finite Element Analyses for Design Evaluation of Biodegradable Magnesium Alloy

- Stents in Arterial Vessels," *Materials Science and Engineering B*, vol. 176, pp. 1733-1740, 2011.
- [66] A. R. Valiboy, B. P. Mwipatayi and K. Sieunarine, "Fracture of a Carotid Stent: An Unexpected Complication," *Society for Vascular Surgery*, pp. 603-606, 2007.
 - [67] S. I. Bernad, E. S. Bernad, T. Barbat, V. Albulescu and R. Susan-Resiga, "Effects of Different Types of Input Waveforms in Patient-Specific Right Coronary Atherosclerosis Hemodynamics Analysis," *International Journal of Design & Nature and Ecodynamics*, vol. 5, no. 2, pp. 1-18, 2010.
 - [68] M. S. Cabrera, C. W. J. Oomens and F. P. T. Baaijens, "Understanding the Requirements of Self-Expandable Stents for Heart Valve Replacement: Radial Force, Hoop Force and Equilibrium," *Journal of the Mechanical Behavior of Biomedical Materials*, vol. 68, pp. 252-264, 2017.
 - [69] A. Azaouzi, N. Lebaal, A. Makradi and S. Belouettar, "Optimization Based Simulation of Self-Expanding Nitinol Stent," *Materials and Design*, vol. 50, pp. 917-928, 2013.
 - [70] R. Fish and L. Geddes, "Conduction of Electrical Current to and Through the Human Body: A Review," *Eplasty*, vol. 9, p. e44, 2009.
 - [71] F. Nematzedah and S. K. Sadrnezhad, "Effects of Material Properties on Mechanical Performance of Nitinol Stent Designed for Femoral Artery: Finite Element Analysis," *Scientia Iranica B*, vol. 19, no. 6, pp. 1564-1571, 2012.
 - [72] X. M. Wang, P. Liu, H. Liang, M. C. Zhang, L. Li and Z. F. Yue, "Analysis of the Whole Implementation Process and Optimization of a Nitinol Superelastic Stent," *Materialwiss. Werkstofftech.*, vol. 50, pp. 44-51, 2019.
 - [73] F. Whitcher, "Simulation of In Vivo Loading Conditions of Nitinol Vascular Stent Structures," *Computers and Structures*, vol. 64, pp. 1005-1011, 1997.
 - [74] P. Y. K. Pang, P. T. L. Chian, Y. L. Chua and Y. K. Sin, "A Survivor of Late Prosthesis Migration and Rotation Following Percutaneous Transcatheter Aortic Valve Implantation," *European Journal of Cardio-Thoracic Surgery*, vol. 41, pp. 1195-1196, 2012.
 - [75] M. Padala, E. I. Sarin, P. Willis, V. Babaliaros and P. Block, "An Engineering Review of Transcatheter Aortic Valve Technologies," *Cardiovascular Engineering Technology*, vol. 1, pp. 77-87, 2010.
 - [76] A. Garcia, E. Pena and M. A. Martinez, "Influence of Geometric Parameters on Radial Force During Self-Expanding Stent Deployment. Application for a Variable Stiffness Stent," *Journal of the Mechanical Behavior of Biomedical Materials*, vol. 10, pp. 166-175, 2012.
 - [77] C. Lally, F. Dolan and P. Prendergast, "Cardiovascular Stent Design and Vessel Stresses: a Finite Element Analysis," *Journal of Biomechanics*, vol. 8, pp. 1574-1581, 2005.
 - [78] F. Gervaso, C. Capelli, L. Petrini, S. Lattanzio, L. D. Virgilio and F. Migliavacca, "On the Effects of Different Strategies in Modelling Balloon-Expandable Stenting

- by Means of Finite Element Method," *Journal of Biomechanics*, pp. 1206-1212, 2008.
- [79] F. Migliavacca, L. Petrini, V. Montanari, I. Quagliana, F. Auricchio and G. Dubini, "A Predictive Study of the Mechanical Behavior of Coronary Stents by Computer Modeling," *Mechanical Engineering and Physics*, vol. 27, pp. 13-18, 2005.
 - [80] R. Balossino, F. Gervaso, F. Migliavacca and G. Dubini, "Effects of Different Stent Designs on Local Hemodynamics in Stented Arteries," *Journal of Biomechanics*, vol. 41, pp. 1053-1061, 2008.
 - [81] N. Foin, E. Alegria, S. Sen, R. Petraco, S. Nijjer, C. Di Mario, D. P. Francis and J. E. Davies, "Importance of Knowing Stent Design Threshold Parameters and Post-Dilation Capacities to Optimise Stent Selection and Prevent Stent Overexpansion/Incomplete Apposition During PCI," *International Journal of Cardiology*, vol. 166, no. 3, pp. 755-758, 2012.
 - [82] M. H. Chao, A. D. C. H. L. Lin, Y. Y. Chen and J. H. Kuang, "The Effect of Plaque and Artery Parameters on Stent Expansion During the Implantation Process," *Life Science Journal*, vol. 10, p. 3, 2013.
 - [83] C. Rogers, D. Y. Tseng, J. C. Squire and E. R. Edelman, "Balloon-Artery Interactions During Stent Placement: A Finite Element Analysis Approach to Pressure, Compliance, and Stent Design as Contributors to Vascular Injury," *Circulation Research*, vol. 84, no. 4, pp. 378-383, 1999.
 - [84] A. Colombo, G. Stankovic and J. Moses, "Selection of Coronary Stents," *Journal of the American College of Cardiology*, vol. 40, pp. 1021-1033, 2002.
 - [85] R. McClean and N. Eigler, "Stent Design: Implications for Restenosis," *Reviews in Cardiovascular Medicine*, vol. 3, pp. S16-S22, 2002.
 - [86] H. Kawamoto, V. F. Panoulas, K. Sato, T. Miyazaki, T. Naganuma, A. Sticchi, F. Figini, A. Latib, A. Chieffo, M. Carlino, M. Montorfano and A. Colombo, "Impact of Strut Width in Periprocedural Myocardial Infarction: A Propensity-Matched Comparison Between Bioresorbable Scaffolds and the First-Generation Sirolimus-Eluting Stent," *JACC: Cardiovascular Interventions*, vol. 8, no. 7, pp. 900-909, 2015.
 - [87] T. Ota, H. Ishii, T. Sumi, T. Okada, H. Murakami, S. Suzuki, K. T. N. Kada and T. Murohara, "Impact of Coronary Stent Designs on Acute Stent Recoil," *Journal of Cardiology*, vol. 64, no. 5, pp. 347-352, 2014.
 - [88] S. Garg and P. W. Serruys, "Coronary Stents: Looking Forward," *Journal of the American College of Cardiology*, vol. 56, no. 10, pp. S43-S78, 2010.
 - [89] A. S. Koh, L. M. Choi, L. L. Sim, J. W. Tan, L. W. Khin, T. Chua, T. Koh and S. Chia, "Comparing the Use of Cobalt Chromium Stents to Stainless Steel Stents in Primary Percutaneous Coronary Intervention for Acute Myocardial Infarction: A Prospective Registry," *Acute Cardiac Care*, vol. 13, no. 4, pp. 219-222, 2011.
 - [90] G. Mani, M. Feldman, D. Patel and C. Agrawal, "Coronary Stents: A Materials Perspective," *Biomaterials*, vol. 28, pp. 1689-1710, 2007.

- [91] S. Bangalore, S. Kumar and M. Fusaro, "Short- and Long-Term Outcomes with Drug-Eluting and Bare-Metal Coronary Stents: a Mixed-Treatment Comparison Analysis of 117,762 Patient-Years of Follow-Up from Randomized Trials," *Circulation*, vol. 125, pp. 2873-2891, 2012.
- [92] E. Van Belle, C. Bauters, E. Hubert, J. C. Bodart, K. Abolmaali, T. Meurice, E. P. McFadden, J. M. Lablanche and M. E. Bertrand, "Restenosis Rates in Diabetic Patients: a Comparison of Coronary Stenting and Balloon Angioplasty in Native Coronary Vessels," *Circulation*, vol. 96, no. 5, pp. 1454-1460, 1997.
- [93] D. Stoekel, A. Pelton and T. Duerig, "Self-Expanding Nitinol Stents: Material and Design Considerations," *European Riology*, vol. 14, pp. 292-301, 2004.
- [94] R. Erbel, C. Di Mario, J. Bartunek, J. Bonnier, B. de Bruyne, F. R. Eberli, P. Erne, M. Haude, B. Heublein, M. Horrigan, D. Ilesley, D. Bose, J. Koolen, T. F. Luscher, N. Weissman and R. Waksman, "Temporary Scaffolding of Coronary Arteries with Bioabsorbable Magnesium Stents: A Prospective, Non-Randomised Multicentre Trial," *The Lancet*, vol. 369, pp. 1869-1875, 2007.
- [95] T. Duerig and M. Wholey, "A Comparison of Balloon and Self-Expanding Stents," *Minimally Invasive Thermal Allied Technology*, vol. 11, no. 4, p. 173, 2002.
- [96] W. Wu, S. Chen, D. Gastaldi, L. Petrini, D. Mantovani, K. Yang, L. Tan and F. Migliavacca, "Experimental Data Confirm Numerical Modeling of the Degradation Process of Magnesium Alloys Stents," *Acta Biomaterialia*, vol. 9, pp. 8730-8739, 2013.
- [97] W. Wu, D. Z. Yang, M. Qi and W. Q. Wang, "Stent Expansion in Curved Vessel and Their Interactions: A Finite Element Analysis," *Journal of Materials Processing Technology*, vol. 184, pp. 447-450, 2007.
- [98] J. A. Grogan, S. B. Leen and P. E. McHugh, "Comparing Coronary Stent Material Performance on a Common Geometric Platform Through Simulated Bench Testing," *Journal of Mechanical Behavior of Biomedical Materials*, vol. 12, pp. 129-138, 2012.
- [99] J. A. Grogan, S. B. Leen and P. E. McHugh, "Optimizing the Design of a Bioabsorbable Metal Stent Using Computer Simulation Methods," *Biomaterials*, vol. 34, pp. 8049-8060, 2013.
- [100] J. A. Grogan, B. J. O'Brien, S. B. Leen and P. E. McHugh, "A Corrosion Model for Bioabsorbable Metallic Stents," *Acta Biomaterialia*, vol. 12, pp. 3523-3533, 2011.
- [101] M. A. Zulliger, P. Fridez, K. Hayashi and N. Stergiopulos, "A Strain Energy Function for Arteries Accounting for Wall Composition and Structure," *Journal of Biomechanics*, vol. 37, pp. 989-1000, 2004.
- [102] K. Van de Graff, Human Anatomy, McGraw-Hill, 2000.
- [103] F. G. P. Welt and C. Rogers, "Inflammation and Restenosis in the Stent Era," *Atherosclerosis, Thrombosis, and Vascular Biology*, vol. 22, pp. 1769-1776, 2002.

- [104] E. Widmaier, H. Raff and K. Strang, *Vander's Human Physiology: the Mechanisms of Body Function*, New York: McGraw-Hill, 2008.
- [105] H. P. Mazumdar, U. N. Ganguly, S. Ghorai and D. C. Dalal, "On the Distributions of Axial Velocity and Pressure Gradient in a Pulsatile Flow of Blood through a Constricted Artery," *Indian Journal of Pure and Applied Mathematics*, vol. 27, no. 11, pp. 1137-1150, 1996.
- [106] S. I. Bernad and E. S. Bernad, "Coronary Venous Bypass Graft Failure, Hemodynamic Parameters Investigation," in *IASTED International Conference Biomedical Engineering*, Innsbruck, Austria, 2012.
- [107] A. Boyd, D. Kuhn, R. Lowzowy and G. Kulbisky, "Low Wall Shear Stress Predominates at Sites of Abdominal Aortic Aneurysm Rupture," *Journal of Vascular Surgery*, vol. 63, no. 6, pp. 1613-1619, 2016.
- [108] Z. Tyfa, D. Obidowski, P. Reorowicz, L. Stefanczyk, J. Fortuniak and K. Jozwik, "Numerical Simulations of the Pulsatile Blood Flow in the Different Types of Arterial Fenestrations: Comparable Analysis of Multiple Vascular Geometries," *Biocybernetics and Biomedical Engineering*, vol. 38, pp. 228-242, 2018.
- [109] W. Y. Chan, "Simulation of Arterial Stenosis Incorporating Fluidstructural Interaction and Non-Newtonian Blood Flow," RMIT University, Melbourne, Australia, 2006.
- [110] S. Amornsamankul, B. Wiwattananapataphee, Y. Hong Wu and Y. Lenbury, "Effect of Non-Newtonian Behaviour of Blood on Pulsatile Flows in Stenotic Arteries," *World Academy of Science, Engineering and Technology International Journal of Medical and Health Science*, vol. 1, no. 2, pp. 108-112, 2007.
- [111] B. Wiwattananapataphee, Y. H. Wu, T. Siriapisith and B. Nuntadilok, "Effect of Branchings on Blood Flow in the System of Human Coronary Arteries," *Mathematical Biosciences and Engineering*, vol. 9, no. 1, pp. 199-214, 2012.
- [112] D. C. Sanyal and A. K. Maiti, "On Steady and Pulsatile Motion of Blood," *Czechoslovak Journal of Physics*, vol. 48, no. 3, pp. 347-354, 1998.
- [113] P. K. Mandal, "An Unsteady Analysis of Non-Newtonian Blood Flow through tapered Arteries with a Stenosis," *International Journal of Non-Linear Mechanics*, vol. 40, no. 1, pp. 151-164, 2005.
- [114] B. Wiwattananapataphee, S. Amornsamankul, Y. Hong Wu and Y. Lenbury, "Non-newtonian Blood Flow Through Stenosed Coronary Arteries," in *Proceedings of the 2nd WSEAS International Conference on Applied and Theoretical Mechanics*, Venice, Italy, 2006.
- [115] D. F. Young and F. Y. Tsai, "Flow Characteristics in Models of Arterial Stenosis - II. Unsteady Flow," *Journal of Biomechanics*, vol. 6, no. 5, pp. 547-559, 1973.
- [116] K. W. Lee and X. Y. Xu, "Modelling of Flow and Wall Behaviour in Mildly Stenosed Tube," *Medical Engineering and Physics*, vol. 24, no. 9, pp. 575-586, 2002.

- [117] V. Deplano and M. Siouffi, "Experimental and Numerical Study of Pulsatile Flows through Stenosis: Wall Shear Stress Analysis," *Journal of Biomechanics*, vol. 32, no. 10, pp. 1081-1090, 1999.
- [118] B. Wiwatanapataphee, "Modelling of Non-Newtonian Blood Flow Through Stenosed Coronary Arteries," *Dynamics of Continuous, Discrete and Impulsive Systems Series B: Applications and Algorithms*, vol. 15, no. 5, pp. 619-634, 2008.
- [119] A. de Bruin, "Numerical Simulation of Bloodflow through Elastic Vessels," Department of Mathematics, University of Groningen, Groningen, 2003.
- [120] W. Quanyu, L. Xiaojie, P. Lingjiao, T. Weige and Q. Chunqi, "Simulation Analysis of Blood Flow in the Arteries of the Human Arm," *Biomedical Engineering*, vol. 29, no. 4, 2017.
- [121] T. Gabe, J. Gault, J. Ross, D. Mason, C. Mills, J. Schillingford and E. Braunwald, "Measurement of Instantaneous Blood Flow Velocity and Pressure in Conscious Man with a Catheter-Tip Velocity Probe," *Circulation*, vol. 40, no. 5, pp. 603-614, 1969.
- [122] C. Rajashekar, G. Manjunatha and B. Fabian, "Finite Element Simulation of Blood Flow Through an Artery Bifurcation: A Mathematical Model," *Malaysian Journal of Mathematical Sciences*, vol. 11, no. 2, pp. 165-179, 2017.
- [123] L. Kallekar, C. Viswanath and M. Anand, "Effect of Wall Flexibility on the Deformation during Flow in a Stenosed Coronary Artery," *Fluids*, vol. 2, no. 2, p. 16, 2017.
- [124] A. P. Singh, "A Framework to Improve Turbulence Models Using Full-field Inversion and Machine Learning," The University of Michigan, Ann Arbor, 2018.
- [125] P. Milani and J. Eaton, "Magnetic Resonance Imaging, Optimization, and Machine Learning to Understand and Model Turbulent Mixing," in *21st Australasian Fluid Mechanics Conference*, Adelaide, Australia, 2018.

Appendix A

Stress-dependent Flexinol Wire Actuation

```
%variables%

d_i=0.000125 %initial diameter%

nu=0.3 %Poisson ratio%

L=0.2 %initial length in meters%

rho=0.00009 %resistivity%

A_i=(pi*(d_i^2))/4 %initial area of the wire%

F_o=2.187 %pull force of the wire%

Sigmamax=F_o/A_i %stress in the wire%

syms Sigma

a_h=0.000002*Sigma^2-0.0009*Sigma+0.6875 %slope coefficient for
heating%

b_h=-0.00005*Sigma^2+0.0203*Sigma-11.927 %intercept coefficient for
heating%

%Coefficients%

A=pi*((d_i)^2)*(nu^2)/(L^2)

B=((d_i^2)*nu/L)*(-(2*pi)-(b_h*nu/L))

C=(pi*(d_i^2))-(4*a_h*rho)+(2*b_h*(d_i^2)*nu/L)

D=(-4*a_h*rho*L)-(b_h*(d_i^2))
```

```
%Governing equation for the actuation of the wire%
```

```
Dh=[A B C D]
```

```
delta_h=roots(Dh)
```

```
%delta_h% %actuation of the wire%
```

```
%A*(delta_h^3)+B*(delta_h^2)+C*delta_h+D=0%
```

```
%Control Equation%
```

```
%Constants%
```

```
alpha=(L^2)/(nu^2)
```

```
beta=(2*rho)/(pi*(d_i^2))
```

```
gamma=2/d_i
```

```
epsilon=(rho^2)/((pi^2)*(d_i^2))
```

```
theta=(nu*rho*(nu+1))/(pi*L)
```

```
%Measured constants%
```

```
R_0M=5.08
```

```
R_0A=4.82
```

```
T_0M=0
```

```
T_0A=225
```

```
dRM_dT=0.00614
```

```
dRA_dT=0.000802
```

```
dRM_dsigma=0.000821
```

```
dRA_dsigma=0.000390
```

```
%Variables%
```

```
sigma=200
```

```
T=(0:1:210)
```

```
%Equations%
```

```
R_M=R_0M+((T-T_0M)*dRM_dT)+(sigma*dRM_dsigma)
```

```
R_A=R_0A+((T-T_0A)*dRA_dT)+(sigma*dRA_dsigma)
```

Biographical Sketch

Matthew Lucci was born in Fort Worth, Texas. After graduating with a homeschool diploma, Matthew studied Mechanical Engineering at Southern Methodist University in Dallas, Texas. While in attendance, Matthew taught or co-taught courses in physics and communication studies while competing on the university debate team. Upon graduation with his Bachelor of Science degree in 2018, he was recruited to coach the debate team at the University of Texas at Tyler. He entered the Master of Science in Mechanical Engineering program at the University of Texas at Tyler in the Fall of 2018.